

**Towards an adenosine wave detection for neuroscience
applications - An aptamer based approach**

Marta Luísa Rodrigues Ornelas

Thesis to obtain the Master of Science Degree in
Biomedical Engineering

Supervisor: Prof. João Pedro Estrela Rodrigues Conde
External Supervisor: Prof. Ana Maria de Sousa Sebastião

Examination Committee

Chairperson: Prof. Patrícia Margarida Piedade Figueiredo
Supervisor: Prof. João Pedro Estrela Rodrigues Conde
Members of the Committee: Prof. Luís Joaquim Pina da Fonseca
Prof. Maria José de Oliveira Diógenes Nogueira

July 2014

To my parents
Aos meus pais

It is our choices that show us who we truly are, far more than our abilities.

J.K. Rowling, *Harry Potter and the Chamber of Secrets*

São as nossas escolhas que nos mostram quem realmente somos, muito mais do que nossas habilidades.

J.K.Rowling, *Harry Potter e a Câmara dos Segredos*

ABSTRACT

Adenosine is known not just as the core molecule of ATP, but also as a neuromodulator. Due to its many functions, through the years it became subject of several studies and extensive research to properly understand its actions, in particular its neuromodulatory role. Despite being recognized as a neuroprotective molecule, the role of adenosine in brain disorders still remains partially unanswered. Gaining knowledge about changes in adenosine levels in different definable extracellular domains in the brain is a step towards a better understanding of adenosine behaviour.

This thesis describes the development of a biosensor based on an aptamer for real time detection and quantification of different concentrations of adenosine.

Aptamers are short single-stranded DNA or RNA molecules that are capable of binding a target with high affinity and specificity selected *in vitro* by SELEX.

In order to develop and optimise a biosensor to detect adenosine, a DNA aptamer labelled with a fluorophore that hybridizes with a single-stranded DNA marked with dabcyI, quenching the fluorescence signal of the aptamer was used. In the presence of adenosine, the aptamer binds with adenosine instead of the DNA with dabcyI, increasing the fluorescence signal.

A macro and microscale analysis was performed. For the microscale analysis, a proper microfluidic was chosen (gradient generator), in order to identify the behaviour of different concentrations of adenosine at the same time. The best value obtained for the limit of detection was 81 μM . In the future, more testing should be undertaken in order further optimise this value.

Key words: Adenosine detection, aptamer, neurosciences, microfluidics.

RESUMO

A adenosina conhecida como uma das principais moléculas de ATP, é também um neuromodulador. Dadas as diversas funções que assume, tem sido ao longo dos anos objeto de vários estudos de modo a compreender corretamente as suas ações, e em particular o seu papel enquanto neuromodulador. Apesar de reconhecida como neuroprotectora, o seu papel em distúrbios mentais permanece por responder. Neste trabalho será descrito o desenvolvimento de um modelo de detecção com base num aptâmero, em tempo real de forma a quantificar diferentes concentrações de adenosina.

Os aptâmeros são moléculas de ADN OU ARN de cadeia simples, curtos e que são capazes de se ligar a um alvo com elevada afinidade e especificidade selecionados *in vitro*, através de SELEX.

De forma a desenvolver e otimizar um biossensor para detetar a adenosina, foi utilizado um aptâmero de ADN, marcado com um fluoróforo, que hibrida com uma cadeia simples de ADN marcado com 4'-dimetilaminoazobenzeno-4-carboxilato (dabcyl), suprimindo o sinal de fluorescência do aptâmero. Na presença de adenosina, o aptâmero liga-se com esta, libertando o ADN marcado com dabcyl, aumentando de fluorescência.

É então apresentada uma análise em macro e micro escala. Para o caso da última, um dispositivo microfluídico adequado foi escolhido (o gerador de gradientes) de forma a proceder a uma identificação correta do comportamento de diferentes concentrações de adenosina, ao mesmo tempo. Após as optimizações, o valor para o limite de detecção de adenosina foi 81 μM . Em trabalhos futuros, devem ser realizados mais testes, de forma a otimizar este valor.

Palavras-chave: Detecção de Adenosina, aptâmeros, neurociências, microfluídica.

ACKNOWLEDGEMENTS

In the end of such a journey, there are a few people that marked my academic path and for whom I am very grateful.

Firstly, I want to thank Professor João Pedro Conde for accepting me into such a challenging project for me and for all the support and incentive during its development. His knowledge is vast and I am very grateful to learn so much with him during these last months.

Secondly, I want to thank Professor Ana Sebastião for the precious knowledge, which was so important during the development of this project.

I also want to thank Narayanan Srinivasan, Ruben Soares and João Tiago for all the patience with me and for all the advice during the development of my project. To Narayanan Srinivasan and Ruben Soares I also want to thank the patience during my first steps in biolab and for the review of this thesis.

I cannot forget my fellows of these last months, Rui Pinto and Catarina Pedrosa who understand better than anyone all my doubts and insecurities. For them, I wish all the best!

My gratitude for my parents is tremendous, since without them I would never have been able to complete such a journey. I thank them for all the love, affection and for always providing me with the best conditions to study without ever pressuring me or demanding anything in return.

I also thank all my family, in particular Tia Guida, Tio Dinis, Diogo and Valentina, for all the good moments when I was home and that always give me strength to carry on.

To my best friend, the sister I never had and my roommate for so many years, Joana Ribeiro I want to express my full gratitude for always believing in me and for all the support during these years, and more recently for the patience to read this thesis. We shared the best and the worst during our journey in Lisbon and that deeply impacted my growth as a person.

I also want to thank all my colleagues that marked my entire journey during these past seven years, particularly to my closest friends: Martas (Santos, Borralho and Farracho). I thank Marta Borralho for the patience to read this thesis.

I also want to thank Tatiana Sirgado, Andreia Duarte, Vasco Duarte, Rafael Gonçalves, Tiago Malaquias, Pedro Chagas and Francisco Martinho. They were definitely some of the people that I will always remember and for whom I wish all the best.

A special thank you to my roommates this last year, Cláudia and Joana, who were so supportive during all this process and always helped when I asked. In particular to Cláudia, for the friendship and for the all the time we spent together studying and battling against Técnico.

Last, but not the least, I want to thank João, for being such a wonderful person, and a supportive and patient boyfriend. For always believing in me and in what I am capable of and for all the help during these last months.

CONTENTS

Abstract	i
Resumo	iii
Acknowledgements	v
Contents	vii
List of Figures	ix
Acronyms	xiii
Motivation	1
Thesis Outline	3
1 Introduction	5
1.1 Adenosine.....	6
1.1.1 Pathways of adenosine production, metabolism and transport	6
1.1.2 Receptors of Adenosine.....	7
1.1.3 Adenosine, a case of study	8
1.2 Aptamers	9
1.2.1 The SELEX Method	10
1.2.2 Aptamers as a biosensor	11
1.2.3 Immobilization of Aptasensors	12
1.2.4 Aptasensors for adenosine	14
1.3 Microfluidics	16
1.3.1 Gradient Generator	17
2 Methodology	21
2.1 Macro scale	22
2.1.1 Quantification of ratio between Aptamer and ssDNA-Q	22
2.1.2 Detection of adenosine	22
2.2 Micro scale.....	23
2.2.1 Gradient Generator	23

2.2.2	Tests in the Gradient Generator with Aptamer and ssDNA-Q.....	25
2.2.3	Tests with adenosine using a Microfluidic Structure.....	27
2.2.4	Immobilization of the Aptamer	28
3	Results and Discussion	31
3.1	Molecular Interaction between ssDNA-Q and Aptamer.....	32
3.1.1	Tris-EDTA (TE) Buffer.....	32
3.1.2	HEPES Buffer	34
3.1.3	Astrocytes Buffer.....	35
3.1.4	Comparing Intensity of Fluorescence of Aptamer for different Buffers.....	36
3.2	Behaviour of Aptamer and ssDNA-Q in the presence of adenosine	37
3.3	The Gradient Generator and the behaviour of Aptamer, ssDNA-Q and Adenosine	40
3.3.1	Functionalization of the Gradient Generator and Control Test with Aptamer and ssDNA-Q.....	41
3.3.2	Adenosine Behaviour in the Gradient Generator.....	45
3.4	Towards physiological concentrations of adenosine in the Gradient Generator	50
3.4.1	Immobilization of the Aptamer	54
4	Conclusions and future work.....	57
	Bibliography	61
	Appendixes	65

LIST OF FIGURES

Chapter 1 Introduction

Figure 1.1. Chemical Structure of Adenosine.....	6
Figure 1.2. Intra and Extra-cellular ATP/Adenosine Signalling Cascades. (Chikahisa & Séj, 2011)	7
Figure 1.3. Distribution of high affinity adenosine receptors (A_1 , A_{2A} and human A_3) in the main regions of the central nervous system. (Ribeiro and Sebastião 2003)	8
Figure 1.4. SELEX Process.....	11
Figure 1.5. Electrochemical aptasensor using MB (Methylene Blue). In the presence of the target, the aptamer folds into the target-binding three-way junction, altering the electron transfer (eT) and increasing the observed reduction peak. (Song, Lee, & Ban, 2012).....	12
Figure 1.6. Optical aptasensors using Fluorescence. The target binding induces an antisense displacement and results in an increase in fluorescence. (Song, Lee, & Ban, 2012)	12
Figure 1.7. Main immobilization procedures for Aptamers.....	13
Figure 1.8. Two-step procedure for direct formation of aptamer mixed monolayers on gold. (Balamurugan & Obubuafo, 2007)	14
Figure 1.9. Schematic illustration of an aptasensor based on home-made europium. (Adapted from (Huang, Niu, Zeng, & Ruan, 2011)).....	15
Figure 1.10. Scheme of the design of the adenosine sensor based on terbium complex (Tb) conjugated to a DNA aptamer. (Li , Ge, Selvin, & Lu, 2012).....	15
Figure 1.11. Soft-Lithography Process. (Adapted from (Scullion, Krauss, & Di Falco, 2013))	16
Figure 1.12. Gradient Generator (Dertinger, Chiu, Jeon, & Whitesides, 2001).	18
Figure 1.13. Junction of two serpentes with different colours brought together. The colour of the mixed channel was rapidly homogenized (Jeon, et al., 2000).	18
Figure 1.14. Schematic Representation of Gradient Generator and Examples of the Gradient Generator used. In the scheme it is also possible to see how B and V values are distributed.....	19
Figure 1.15. Splitting Ratios for a structure with 3 inlets.	19
Figure 1.16. Schematic demonstration of calculations in branching points. C_p , C_q and C_r represents the incoming streams. (Dertinger, Chiu, Jeon, & Whitesides, 2001).....	20

Chapter 2 Methodology

Figure 2.1. Aptasensor for Adenosine. Aptamer for adenosine marked with a Green Fluorophore which is initially bond with a ssDNA-Q with a Dabcyl (red dot) – No fluorescence detected. In the presence of adenosine, the Aptamer is more stable with this molecule and connects with adenosine instead of the ssDNA-Q – the fluorescence increases. (Adapted from (Elowe, et al., 2006))	21
Figure 2.2. Gradient Generator scheme, with detail of serpentine where the mixes occur and the chambers. (Adapted from (Fernandes, Gameiro, Tenreiro, Chu, & Outeiro, 2013))	23
Figure 2.3. Moulds on a Petri Dish, ready to pour PDMS.	24
Figure 2.4. PDMS device ready to use.	25
Figure 2.5. Syringe pump during the process of functionalization of the PDMS device with BSA-1%.	26
Figure 2.6. Inlets of the Gradient Generator. Inlet 1 corresponds to the solution with 500 nM Aptamer, Inlet 2 corresponds to the solution with 500 nM Aptamer and 1000 nM ssDNA-Q and Inlet 3 corresponds to 500 nM Aptamer and 2000 nM ssDNA-Q.	26
Figure 2.7. Setup of the Experiments using the gradient generator, in the Microscope.	28

Chapter 3 Results and Discussion

Figure 3.1. Comparison of Fluorescence between different concentrations of Aptamer and ssDNA-Q, using TE Buffer.	33
Figure 3.2. Fluorescence intensity of 500 nM Aptamer with different concentrations of ssDNA-Q, using TE-Buffer.	33
Figure 3.3. Fluorescence intensity of 500 nM Aptamer with different concentrations of ssDNA-Q, using HEPES Buffer.	35
Figure 3.4. Fluorescence intensity of 500 nM Aptamer with different concentrations of ssDNA-Q, using Astrocytes Buffer.	36
Figure 3.5. Fluorescence Comparison between the three Buffers. (500 nM Aptamer and different concentrations of ssDNA)	37
Figure 3.6. Fluorescence intensity of 500 nM Aptamer and 1000 nM ssDNA-Q with different concentrations of Adenosine, using HEPES Buffer.	38
Figure 3.7. Fluorescence intensity of 500 nM Aptamer and 1000 nM ssDNA-Q with different concentrations of Adenosine, using Astrocytes Buffer.	38
Figure 3.8. Behaviour of Adenosine according to a Langmuir Model	39
Figure 3.9. Values for the calculation of Limit of Detection for each Buffer.	40
Figure 3.10. Theoretical Values for each Chamber of the Gradient Generator.	42
Figure 3.11. Outlet of the Gradient Generator and a Profile Plot from ImageJ.	42
Figure 3.12. Illustrative Picture of the 9 Chambers, concentrations from each inlet and expected values of ssDNA-Q are represented on the table.	43

Figure 3.13. Fluorescence Intensity for 500 nM of Aptamer and various concentrations of ssDNA-Q, in PDMS device. Each point represents a different chamber.	44
Figure 3.14. Comparison of Fluorescence for 500 nM of Aptamer and different concentrations of ssDNA-Q in Astrocytes Buffer in Micro and Macro scale.	45
Figure 3.15. Relative concentration for each chamber of the PDMS device. The highlight cells of the table correspond to the concentration of adenosine from each solution prepared. All the three solutions contained the mix of 500 nM Aptamer and 1000 nM ssDNA-Q.	46
Figure 3.16. Intensity for different concentrations of Adenosine with 500 nM Aptamer and 1000 nM ssDNA-Q. Conditions of acquisition: 1s Exposure and 2x Gain.	46
Figure 3.17. Intensity for different concentrations of Adenosine with 500 nM Aptamer and 1000 nM ssDNA-Q. Conditions of acquisition: 1s Exposure and 2x Gain.	47
Figure 3.18. Comparison of the common relative concentrations of the two tests with Adenosine. The results are normalized to the intensity value of 500 nM Aptamer (without adenosine and ssDNA-Q).	48
Figure 3.19. Outlets of PDMS Devices. a) Inlet 1: Aptamer (500 nM) + ssDNA-Q (1000nM) Inlet 2: Aptamer (500 nM) + ssDNA-Q (500 nM) Inlet 3: Aptamer (500 nM) b) 3 inlets with same concentration of Aptamer and ssDNA-Q (500 nM and 1000 nM) e different concentrations of adenosine (Inlet 1: 500 μ M; Inlet 2: 250 μ M; Inlet 3: 0 μ M) c) 3 inlets with same concentration of Aptamer and ssDNA-Q (500 nM and 1000 nM) e different concentrations of adenosine (Inlet 1: 250 μ M; Inlet 2: 125 μ M; Inlet 3: 0 μ M). Conditions of acquisition: 2x Gain and 1s Exposure.	49
Figure 3.20. Outlet of PDMS Device, with 125 nM Aptamer and different concentrations of ssDNA-Q.	51
Figure 3.21. Concentrations of Aptamer, ssDNA-Q and adenosine for each test.	51
Figure 3.22. Fluorescence Intensity for 500 nM of Aptamer and various concentrations of ssDNA-Q, in PDMS device. Each point represents a different chamber. Acquisition conditions: 2s Exposure 5x Gain	52
Figure 3.23. Intensity for different concentrations of Adenosine with 250 nM Aptamer and 500 nM ssDNA-Q. Conditions of acquisition: 2s Exposure and 5x Gain.	53
Figure 3.24. a) and b) Immobilization of the Aptamer and its Schematic. c) and d) Aptamer immobilized binding with ssDNA-Q and its schematic.	55

Chapter 4

Conclusions and Future Work

Figure 4.1. Actual Approach vs. Future Approach to detect adenosine.	59
---	----

ACRONYMS

ADA	Adenosine Deaminase
ADP	Adenosine diphosphate
AK	Adenosine Kinase
APTES	3-Aminopropyl)triethoxysilane
AR	Adenosine Receptors
ATP	Adenosine triphosphate
BSA	Bovine Serum Albumin
cAMP	Cyclic adenosine monophosphate
CNS	Central Nervous System
Dabcyl	4'-dimetilaminoazobenzene-4-carboxilato
DNA	Deoxyribonucleic Acid
EDTA	Ethylenediaminetetraacetic Acid
FAM	Fluorescein amidite
HEPES	4-(2-hydroxyethyl-1-piperazineethanesulfonic acid)
LoD	Limit of Detection
PBS	Phosphate Buffered Saline
PDMS	Polydimethylsiloxane
RNA	Ribonucleic Acid
SELEX	Systematic Evolution of Ligands by Exponential Enrichment
ssDNA	Single Strand Deoxyribonucleic Acid
Tris	Tris(hydroxymethyl)aminomethane)

MOTIVATION

Over the years, adenosine has been the object of numerous studies and extensive research. Recognised as the core molecule of ATP and nucleic acids, its relation to energy metabolism is obvious: under conditions of energy deficiency, there is an increase in adenosine, which promotes actions that limit respiration, blood and cellular work. As stated by (Newby, 1991), increased neuronal activity, particularly in cases of hypoxia or ischemia, results in markedly elevated levels of adenosine, which reveal its important role in the nervous system. In fact, adenosine is recognized as an endogenous anticonvulsant and neuroprotective molecule. Concerning its neuromodulatory role, it relies on a balanced activation of inhibitory A_1 receptors and facilitatory A_{2A} receptors. This role can be a connection point to understand the role of adenosine in the control of brain disorders: A_1 Receptor acts as a hurdle that needs to be overcome to begin neurodegeneration and, in contrast, the blockade of A_{2A} Receptors alleviates the long-term burden of brain disorders in different conditions, such as ischemia, epilepsy, Parkinson's or Alzheimer's diseases.

As reported by (Gomes , Kaster , Tomé , Agostinho, & Cunha, 2011), these two receptors of adenosine may potentially be manipulated, although several uncertainties are associated with the process and the role of adenosine in the control of brain disorders is yet to be fully understood. Furthermore, the authors also report that many questions related with the metabolism of adenosine remain unanswered. In fact, they believe that knowing when, where, and how the extracellular levels of adenosine are changing in different definable extracellular domains in the brain is fundamentally important to predict the impact of manipulating the adenosine modulation system.

The main motivation for this project was to monitor the space and time variations in concentration of extracellular adenosine resulting from neuronal activity. This project is a step towards the quantification of the extracellular adenosine with high temporal and spatial resolution. Since there is no reported technique for this quantification, a new model was designed. The conditions for the system are simple: real time detection and quantification of different concentrations of adenosine.

Based on the latest techniques to detect small molecules such as adenosine, a study of different biosensors with particular highlight in aptamers was made. The focus given to aptamers is due to the fact that these are an emergent tool to detect small molecules and have many advantages compared, for example, to antibodies.

This thesis constitutes one more step towards the detection of the adenosine wave, by developing a system that is sensitive to physiological concentrations of adenosine.

THESIS OUTLINE

This work will be divided into four main chapters:

1. Introduction
2. Methodology
3. Results and Discussion
4. Conclusions and Future Work

In the first chapter, the main concepts behind the work developed throughout this thesis are presented and briefly explained. The main sections in this chapter are a brief introduction about adenosine, an exposition of the emerging technology of aptamers, and a theoretical presentation of microfluidics.

The methodology chapter is divided in two main sections: macroscale and microscale. It consists of a brief description of the main protocols implemented during the experimental work (including all procedures) and of the equipment used.

Furthermore, the third chapter includes a brief analysis of the main results obtained along this experimental work. This analysis is divided into four main sections: two sections for macroscale and two sections for microscale. The first section is a brief analysis of the behaviour of ssDNA-Q and Aptamer in the presence of different buffers. The second section reports the behaviour of Aptamer and ssDNA-Q in the presence of adenosine. Additionally, the third section discusses the behaviour of Aptamer and ssDNA-Q but in a microfluidic device. The last section reports all the efforts made to optimize the system in order to achieve the desirable concentration of adenosine.

Finally, the last chapter includes conclusions of all the work carried as well as some concerns and suggestions to continue developing this work.

1 INTRODUCTION

Adenosine is known as a core molecule of ATP as well as a neuromodulator. Over the years, studies about the behaviour about this molecule have increased but some questions still remain unanswered. One of those questions is related to the metabolism of adenosine and the lack of knowledge due to extracellular levels of adenosine in different definable extracellular domains in the brain. In pursuit of an answer, the development of a biosensor seems to be promising. With this question in mind, aptamers seems to be the best approach. This emergent new class of molecules are presented with a great potential to rival the antibodies in many fields such as in therapeutic and diagnostic as well as basic research applications. Since the main goal of this project is to detect low concentrations of adenosine, a microfluidic approach to perform the experiments is the best choice. Furthermore, microfluidics present many advantages such as the use of small volumes and low energy consumption.

This first chapter, will be a theoretical introduction to the three main points of this work (adenosine, aptamers and microfluidics), and each of them will be explored in three different sections. In the first section, some basic concepts about adenosine will be presented such as its importance, metabolism, pathways as well a brief reference to its receptors and a short review of some case studies related to the influence of adenosine in brain diseases.

Additionally, and since it is the chosen approach to detect adenosine, the second section will be a short explanation about aptamers, its origin and how they are synthesized. Moreover, aptamers' role as a biosensor will also be explained, as well as how they can be immobilized and what type of approaches using the aptamers are available to the adenosine.

On the third section, basic concepts related with microfluidics will be presented with particular prominence on a theoretical understanding of the microfluidic device that will be more used in development of this work, which is the Gradient Generator.

1.1 Adenosine

Adenosine (Figure 1.1) is a nucleoside formed by adenine (a purine) connected to the ribose (carbohydrate) through a glycosidic bond. It is believed to be released by most cells, including neurons and glial cells. However, it is not considered a neurotransmitter since it is neither stored in vesicles nor released like classical neurotransmitters, as stated in (Sebastião & Ribeiro, 2000).

This nucleoside modulates brain function, acting as modulator of modulators (e.g. ATP) and controls synaptic activity acting independently on the three levels of tripartite synapses:

- regulating neurotransmitter release (presynaptically),
- modulating neurotransmitter actions (postsynaptically),
- affecting neurotransmitter uptake and release from astrocytes (perisynaptically) (Sebastião & Ribeiro, 2009).

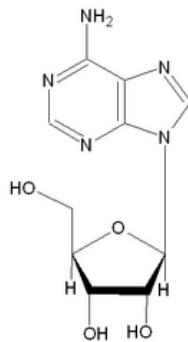


Figure 1.1. Chemical Structure of Adenosine

1.1.1 Pathways of adenosine production, metabolism and transport

According to (Ribeiro, Sebastião, & de Mendonça, 2003), adenosine can be formed extracellularly through two sources:

- Release of adenosine by facilitated diffusion
- Extracellular conversion of released adenine nucleotides into adenosine through a series of ectoenzymes.

A potential source of extracellular adenosine is adenosine nucleotides, which can be extracellularly converted into adenosine by ectonucleotidases (Fredholm, Ijzerman, Jacobson, Klotz, & Linden, 2001). When formed intracellularly, its concentration is dependent on a key enzyme, called adenosine kinase (AK), which is present in most cell types, including neurons and glia (Sebastião & Ribeiro, 2009) (Figure 1.2).

Under normal conditions, adenosine is continuously formed extra and intracellularly (Fredholm, Ijzerman, Jacobson, Klotz, & Linden, 2001). This purine is mainly regulated through its bidirectional transport. Adenosine transporters can be classified in two types (Jarvis & Young, 1986):

- Equilibrative Transporters: transports adenosine according to its gradient concentration. These transporters are also divided in two types: sensible to NBMPR (nitrobenziltioinosina) and insensible to NBMPR;
- Concentrative Transporters: transports adenosine against gradient concentration and depending on Na⁺.

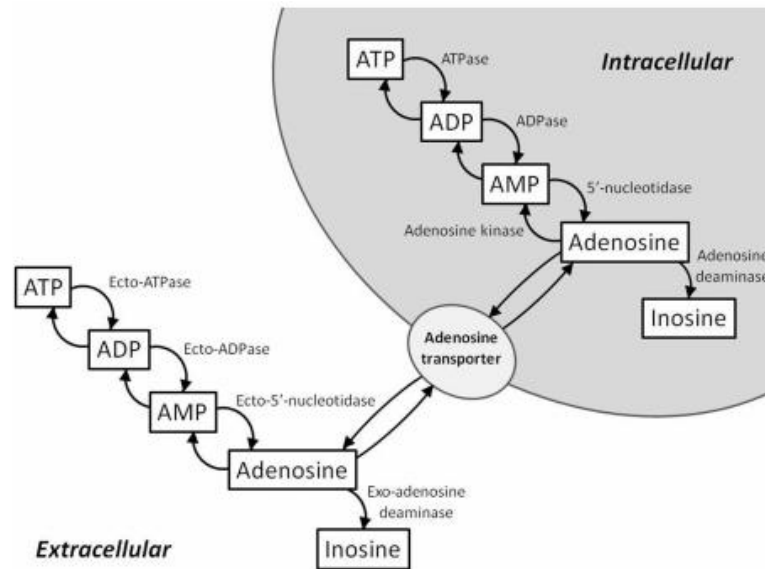


Figure 1.2. Intra and Extra-cellular ATP/Adenosine Signalling Cascades. (Chikahisa & Séi, 2011)

1.1.2 Receptors of Adenosine

Adenosine acts via four sub-types of receptors: A₁, A_{2A}, A_{2B} and A₃. The receptors A₁ and A₃ are negatively coupled to the enzyme adenylate cyclase, decreasing the concentration of intracellular cAMP. On the other hand, the receptors A_{2A} and A_{2B} are positively coupled to the same enzyme, having the opposite effect on the intracellular cAMP. The receptors with the highest affinity for adenosine are A₁ and A_{2A} and the one with lowest affinity is A_{2B}. Receptor A₃ also has a high affinity for adenosine in humans, but, as shown below, it has low density in most tissues (Ribeiro, Sebastião, & de Mendonça, 2003).

Each receptor is located in a different part of the Central Nervous System (Figure 1.3):

- Receptor A₁ is present in the entire CNS, with a higher concentration in the neocortex, hippocampus and cerebellum;
- Receptor A_{2A} is present in the striatum and olfactory bulb;
- Receptor A₃ can be found in low concentrations on the hippocampus, cerebellum and striatum.

Besides its presence in the CNS, adenosine receptors can also be found in the peripheral nervous system, both in the autonomic and the somatic nervous system (Ribeiro, Sebastião, & de Mendonça, 2003).

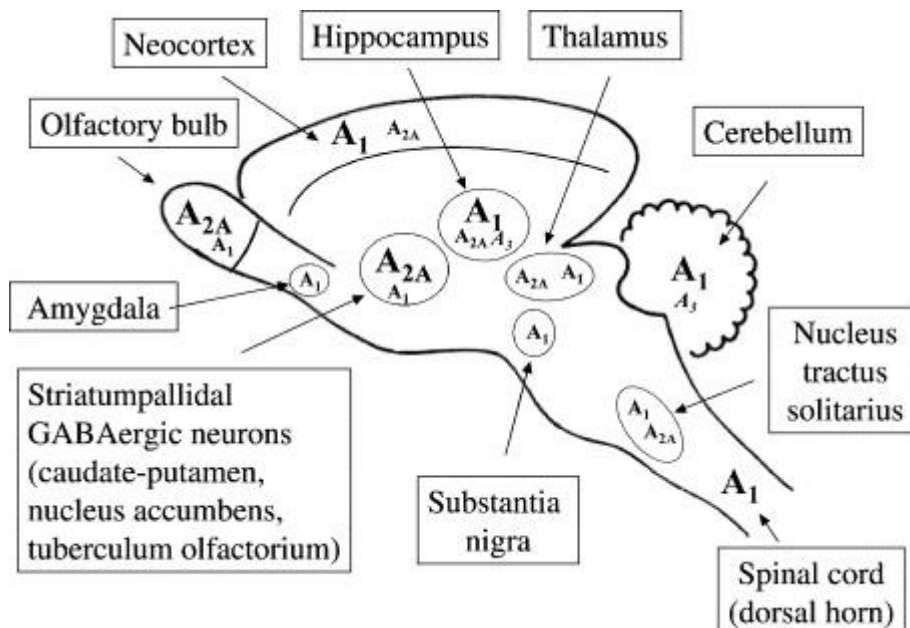


Figure 1.3. Distribution of high affinity adenosine receptors (A₁, A_{2A} and human A₃) in the main regions of the central nervous system. (Ribeiro and Sebastião 2003)

1.1.3 Adenosine, a case of study

Throughout the years, the number of studies and publications about adenosine and adenosine receptors has increased. Particular emphasis has been given to nervous system pathologies and novel therapeutic approaches. In fact, after two or three decades of studies in animals, it was completely established that adenosine receptors are involved in several pathophysiological conditions and with proper manipulation they might be therapeutically useful. Research on humans has been increasing, with a greater focus on sleep, Parkinson's disease and epilepsy.

In 2011, (Porkka-Heiskanena & Kalinchuk, 2011) stated that adenosine may be a final common pathway for various sleeping pattern related factors. In fact, they discovered an increase in adenosine in the basal forebrain during sleep deprivation, which induces sleep. The authors also affirm that adenosine may play a role in the local regulation of sleep homeostasis.

Additionally, (Boison, 2012) states that, among other effects, adenosine deficiency is a pathological hallmark of the epileptic brain. Since some models of epilepsy are resistant to conventional antiepileptic drugs, the author believes that triggering an increase in adenosine in the brain may constitute a powerful approach for seizure prevention. Nevertheless, this triggering might be useful to reconstruct homeostatic functions of the adenosine system only, as (Boison, 2012) concluded in the same article. Furthermore, Boison alerts us to some important points for future work:

- Identification of the mechanisms by which adenosine can affect network changes and disease progression in epilepsy,
- Clinical trials to test the safety and feasibility of focal adenosine accrual for epilepsy.

In 2013, (Aronicaa, Sandau, Iyer, & Boison, 2013) highlights the importance of a therapy consisting on an increase in adenosine for clinical use, arguing that this may revolutionize the neurocentric approach to the treatment epilepsy.

As mentioned before, besides epilepsy and sleep, another focus of study is Parkinson's disease (PD). Since the treatment of PD is largely unsatisfactory, the demand for new therapies is urgent. The new approach must be based in non-dopaminergic therapy, since the dopaminergic chronic therapy has several side effects such as "on/off", "wearing off" and dyskinesia.

There is no doubt of the importance of adenosine and its different receptors in different areas of science, and in particular in neurosciences. The creation of a system that can detect and quantify in real time is an urgent issue. A brief research for emerging biosensors bring us to the aptamers.

1.2 Aptamers

The term aptamer is derived from the Latin word "aptus", which means fitting, and the Greek word "meros", meaning particle (Stoltenburg, Reinemann, & Strehlitz, 2007). Aptamers are oligonucleotides, such as ribonucleic acid (RNA) and single-strand deoxyribonucleic acid (ssDNA) or a combination of these with non-natural nucleotides capable of adopting three dimensional structures which interact precisely and specifically with a target molecule (Smuca, Ahnb, & Ulrichb, 2014). Especially, RNA and ssDNA aptamers can differ from each other in sequence and folding pattern, although they bind the same target (Song, Lee, & Ban, 2012).

This concept began to emerge in the 1980s, from basic science studies of viruses and early work in gene therapy. The first studies focused on the research of human immunodeficiency virus (HIV) and adenovirus. It indicated that these viruses encode a number of small structured RNAs that bind to viral or cellular proteins with high affinity and specificity (Song, Lee, & Ban, 2012).

This observation suggested that RNA ligands might also be useful for therapeutic ends; this motivated gene therapy researchers to start their own studies.

The first one was to determine if an RNA aptamer could be used to inhibit the activity of a pathogenic protein and it was published in 1990 by Sullenger et al. This work demonstrated that the trans-activation response (TAR) aptamer evolved by HIV to recruit viral and cellular proteins to viral transcripts can be turned against the virus to inhibit HIV replication (Dollins, Nair, & Sulle, 2008).

In the same year, Gold's group and Szostak's group reported a new *in vitro* selection process called Systematic Evolution of Ligands by Exponential enrichment (SELEX) (Ellington & Szostak, 1990) (Tuerk & Gold, 1990). Since then, SELEX has consistently been redeveloped, and today it is considered a basic technique for the isolation of aptamers.

There are many studies of aptamers as bio-material in numerous investigations concerning their use as a diagnostic and therapeutic tool and biosensing probe, and in the development of new drugs, drug delivery systems, disease diagnosis, bio-imaging, analytical reagent, hazard detection and food inspection.

With so many applications, aptamers can be a substitute for antibodies, which have been the most popular class of molecules for molecular recognition in a wide range of application for more than three decades.

Aptamers have many advantages when compared to antibodies. (Lee , et al., 2008) describes some of them:

- High affinity and exquisite specificity
- Can be massively synthesized via chemical progress – the cost for fabrication of aptamer-based biosensors could be cut down.
- Can be easily modified chemically
- More robust at high temperatures, and thermal denaturation of aptamers is reversible.
- The binding of aptamers with their targets usually relies on specific conformations
- Aptamers could interact with other RNA or DNA molecules such as DNAzymes, because of their oligonucleotide nature.
- Nucleic acid aptamers can hybridize with their complementary sequences

With so many advantages, aptamers are considered a good alternative to antibodies in many biological applications.

1.2.1 The SELEX Method

SELEX (Systematic Evolution of Ligands by Exponential Enrichment) as cited above has been introduced by Gold and Szostak as a powerful tool for the *in vitro* selection technique for the generation of aptamers. SELEX (Figure 1.4) is an iterative process in which highly diverse synthetic nucleic acid libraries are selected over many rounds to finally identify aptamers with the desired properties (Schutze, et al., 2011). This process involves a combinatorial library of synthetic oligonucleotides consisting of a multitude of ssDNA fragments (approximately 10^{15}) with different sequences. Gopinath (Gopinath, 2007) describes the process in three main steps:

1. Selection of ligand sequences that bind to a target
2. Partitioning of aptamers from non-aptamers via affinity methods
3. Amplification of bound aptamers

Step 1 involves designing the pool for conventional SELEX, and in this process there are four important factors: the type of randomization; the length of the random sequence region; the chemistry of the pool and the utility of the constant regions. Usually, the selection process starts with a low ratio of nucleic acid to protein in order to check whether all of the molecules bind with the target (Gopinath, 2007).

The amplified molecules are used in the next round of selection processes. Gopinath (Gopinath, 2007) states that the first rounds of selection need longer incubation times and less stringent conditions; later cycles involve more stringent conditions – changing the buffer, reaction volume and time of incubation.

Finally, to complete the entire selection process there are at least 12 cycles (Gopinath, 2007) and after that, the selected sequences can be cloned and sequenced.

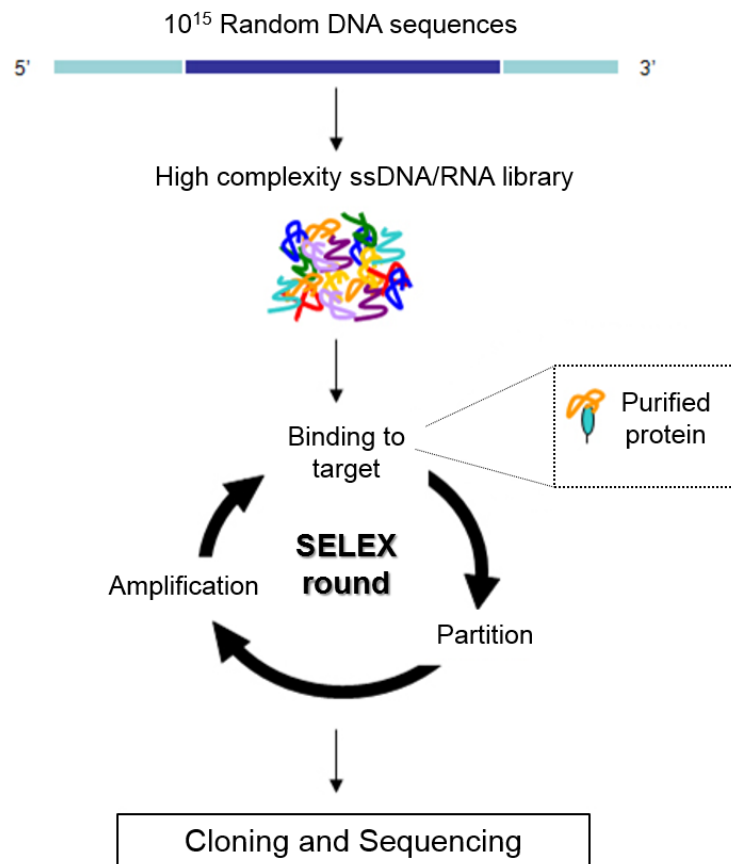


Figure 1.4. SELEX Process

1.2.2 Aptamers as a biosensor

A biosensor, as per definition of the IUPAC (International Union of Pure and Applied Chemistry), is an integrated receptor-transducer device, which is capable of providing selective quantitative or semi-quantitative analytical information (Strehlitz, Nikolaus, & Stoltenburg, 2008). Furthermore, a biosensor that is based on aptamers as a recognition element is called an aptasensor (Song, Lee, & Ban, 2012).

This kind of biosensor can be assembled through a variety of methodologies, of which three types can be highlighted (Song, Lee, & Ban, 2012):

- Electrochemical aptasensor, offers high sensitivity and compatibility with novel microfabrication technologies, inherent miniaturization and low cost (Song, Lee, & Ban, 2012). This biosensor method to obtain the signal transduction includes methods like Faradaic Impedance Spectroscopy (FIS), differential pulse voltammetry, alternating current voltammetry, square wave voltammetry, potentiometry or amperometry (Strehlitz, Nikolaus, &

Stoltenburg, 2008). Figure 1.5 represents an example of this methodology, using MB (Methylene Blue) as an electroactive reporter for signal transduction.

- Optical aptasensor, comprises, for example, the utilization of Surface Plasmon Resonance, evanescent wave spectroscopy, as well as fluorescence anisotropy and luminescence detection (Strehlitz, Nikolaus, & Stoltenburg, 2008). In the case of the fluorescence detection, the simplest format is to label the aptamers with both a quencher and fluorophore, which is the method used in this work. (Figure 1.6)
- Mass-Sensitive aptasensor, is the method that can be used to do a label-free detection of the target (Strehlitz, Nikolaus, & Stoltenburg, 2008). This biosensor uses microgravimetric method on piezoelectric quartz crystals base ion the change of the crystal upon mass change at its surface due to receptor-target binding.

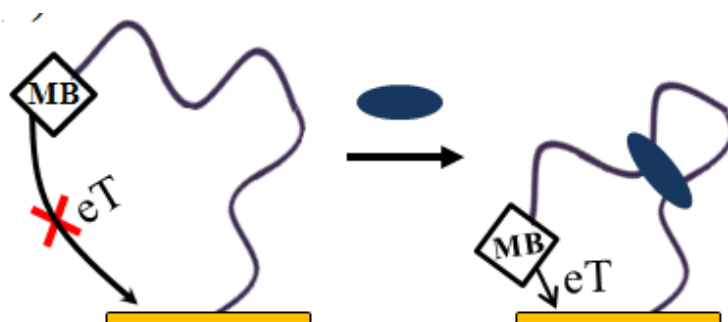


Figure 1.5. Electrochemical aptasensor using MB (Methylene Blue). In the presence of the target, the aptamer folds into the target-binding three-way junction, altering the electron transfer (eT) and increasing the observed reduction peak. (Song, Lee, & Ban, 2012)

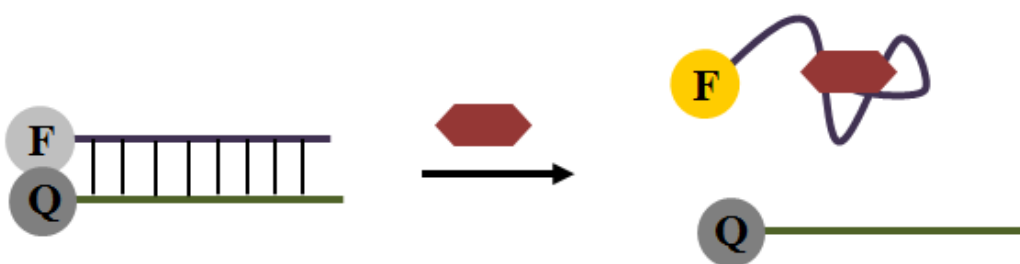


Figure 1.6. Optical aptasensors using Fluorescence. The target binding induces an antisense displacement and results in an increase in fluorescence. (Song, Lee, & Ban, 2012)

1.2.3 Immobilization of Aptasensors

For aptasensors to detect in an effective way, they must have excellent selectivity, accuracy and stability. As (Lim, Kouzani, & Duan, 2009) stated, the immobilization procedure plays a major role in optimizing sensor sensitivity and specificity. There are many procedures for immobilization of

aptamers, mainly based on the ones developed for DNA. Figure 1.7 shows a diagram with the main procedures used.

The procedure chosen for immobilizing the aptamer will have direct influence over the orientation of the aptamer on the surface, as well as on its selectivity and binding affinity. Each procedure depends on the chemical composition of the surface, the availability of suitable aptamer linkers and the chemistries employed for the attachment (Balamurugan & Obubuafo, 2007). The large majority of the processes used for immobilization of aptamers are based on methods already developed for immobilization of DNA hybrids and other biomolecules. The simplest immobilization method is the physical adsorption. The adsorption process is based on ionic, hydrophobic and van der waal's forces. The method is simple: an aptamer solution is placed in contact with the desired surface for a defined period of time and then the surface is washed, to clean the molecules that were not absorbed.

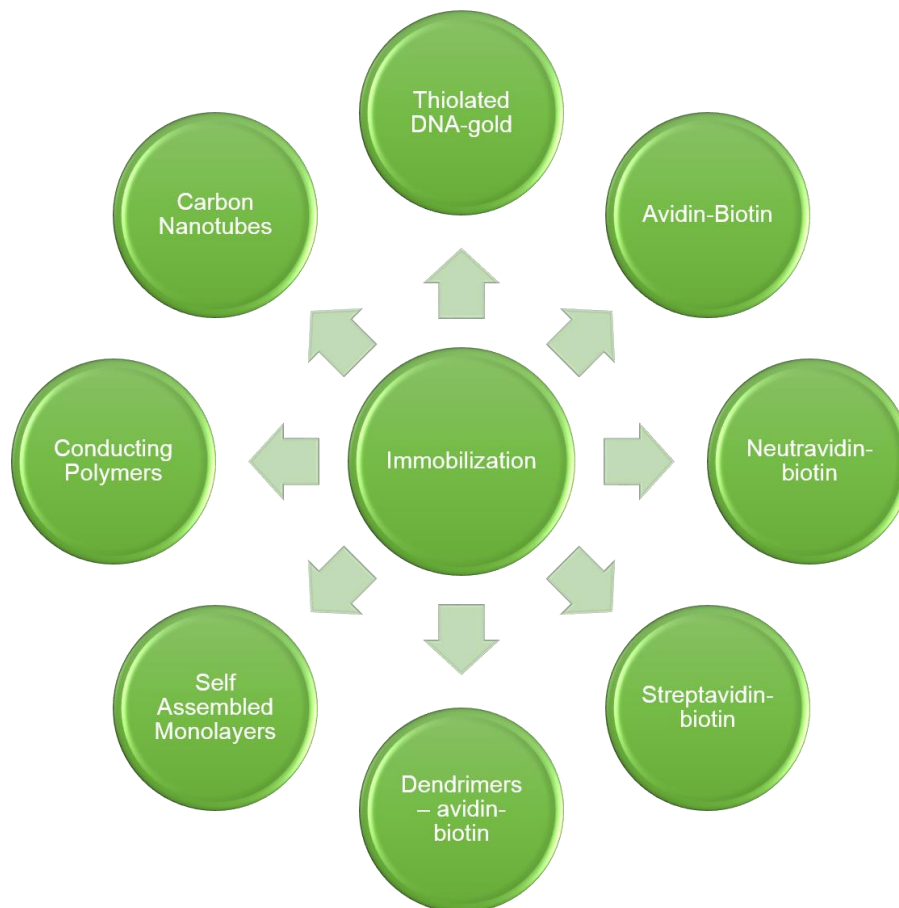


Figure 1.7. Main immobilization procedures for Aptamers.

This simple method presents a weak point, which is biomolecule desorption from the support due to weak and reversible binding. In fact, as described by (Mascini, 2009) the most effective methods are based on:

- chemisorption of thiol-labeled aptamers to a gold surface,
- the strong affinity of biotin to avidin, streptavidin or neutravidin.

The first report of aptasensors in gold was in 2002 by (Liss, Petersen, Wolf, & Prohaska, 2002). The method is typically an immersion of a clean gold substrate in an aqueous buffer solution of thiol-terminated aptamer, which forms a monolayer on the gold surface (Figure 1.8.). The strong affinity of the thiol groups for noble metal surfaces enables the formation of covalent bonds between the sulphur and gold atoms (Sassolas, Blum, & Leca-Bouvier, 2011).

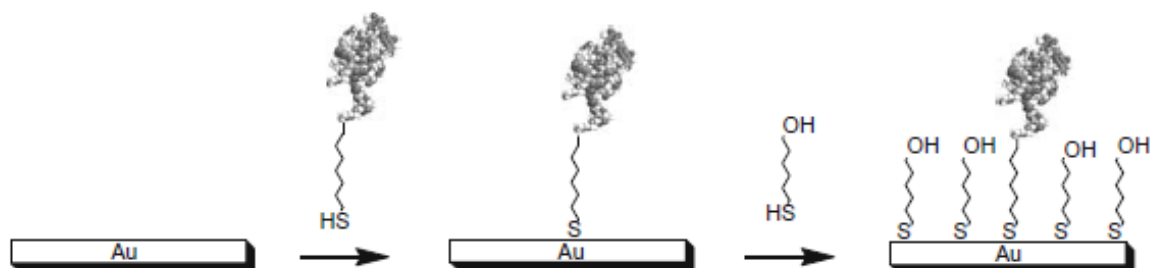


Figure 1.8. Two-step procedure for direct formation of aptamer mixed monolayers on gold.
(Balamurugan & Obubuafu, 2007)

In the second method mentioned, the RNA or DNA aptamer is modified by biotin while the surface is covered by streptavidin, avidin or neutravin (Mascini, 2009). The specific and strong interaction between avidin (or one of its derivatives) and biotin was the starting point for its utilization for aptamer immobilization. As (Sassolas, Blum, & Leca-Bouvier, 2011) stated, biotin is a small molecule that binds with very high affinity to avidin or streptavidin. Furthermore, avidin and streptavidin are tetrameric proteins that have four identical binding site for biotin.

1.2.4 Aptasensors for adenosine

After the introduction of SELEX in 1991, many groups started using *in vitro* selections to isolate RNA and DNA molecules that bind small molecules, such as adenosine. In 1995, David E. Huizenga and Jack W. Szostak presented an aptamer that binds adenosine and ATP (Huizenga & Szostak, 1995). This was the first step in the creation of many aptasensors, using different approaches, as described above.

In this section, the main focus will be given to optical aptasensors, since optical analysis has high sensitivity, quick response and is simple to use. One of the most commonly used techniques, and very popular in the scientific community, is Fluorescence. As (Feng, Dai, & Wang, 2014) describes, optical aptasensors can be mainly divided into two types: the ones with labelled fluorescence and the ones with label-free fluorescence.

Since few aptamers are autofluorescent, labelling is normally necessary to have a measurable signal. In 1996, Wang et al., gave us the first reported technique of labelled fluorescence aptasensor for small biomolecules. From that first report, many labelled aptasensors were designed (or re-designed). For adenosine, in particular, it is possible to find a vast quantity of different aptasensors. (Elowe, et al., 2006), for example, reports an approach of a signalling DNA aptamer that reflects the

1.3 Microfluidics

Microfluidics is a branch with high interdisciplinary that studies the design, fabrication and operation of systems of microscopic channels that conduct fluids (Tabling, 2003).

The concept of Microfluidics has its origins on the established concept of MicroElectro-Mechanical Systems (MEMS) in the 80's and in the introduction of biological, chemical and biomedical applications. Microfluidics can be defined as the study of flows that are simple or complex, mono-or multiphasic, which are circulating in the artificial microsystems as stated in (Tabling, 2003).

A microfluidic device is produced by a common process used in the nanotechnology, called soft-lithography. The process is simple and expeditious: polymer is poured into a mould (with patterned relief structures) to create the device (Figure 1.11).

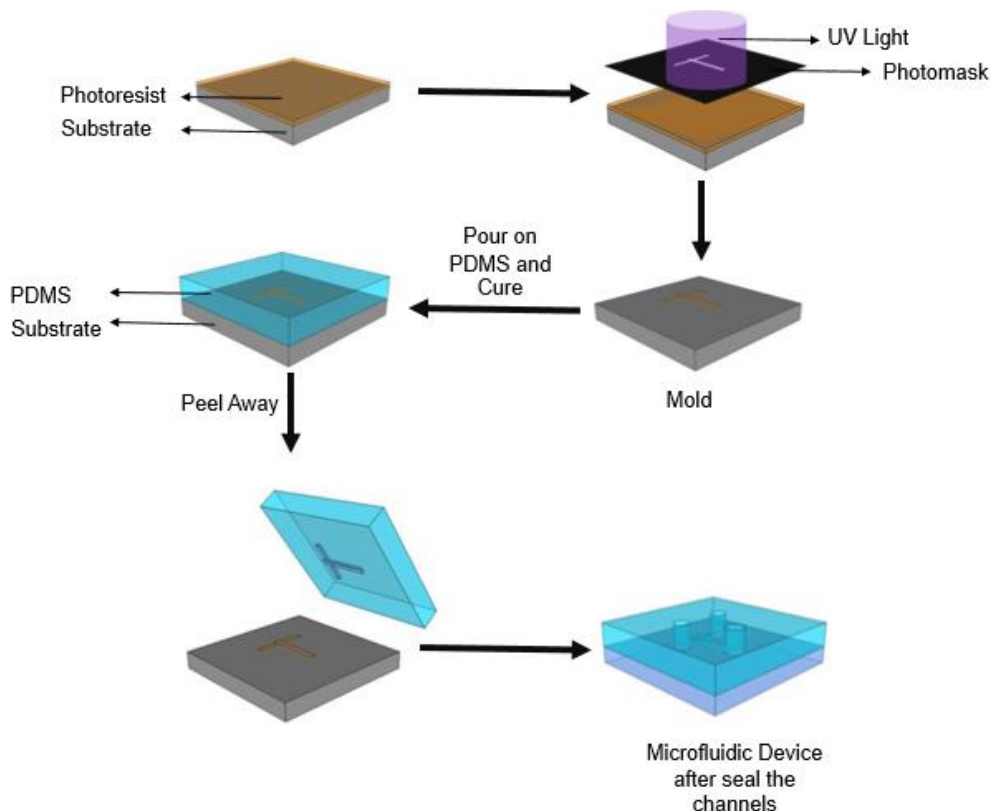


Figure 1.11. Soft-Lithography Process. (Adapted from (Scullion, Krauss, & Di Falco, 2013))

The polymer mentioned above has an important role in these devices. The most commonly used is polydimethylsiloxane (PDMS), a silicon based polymer with the formula $(\text{Si}(\text{CH}_3)_2\text{O})_n$. PDMS when mixed with a curing agent and placed in a temperature beyond its polymerization temperature (around 70°C) is capable of forming an elastomer (Tabling, 2003). There are some characteristics that make PDMS an advantageous polymer for microfluidic structures (Tabling, 2003):

- Optically transparent to wavelengths between 300 and 2200 nm;
- Electrical and thermally insulating;
- Permeable to gas and nearly impermeable to water
- Inert and nontoxic.

As mentioned above, a microfluidic device is produced by a soft-lithography process, which is a convenient, effective and low-cost method, with a resolution from 30 nm to 100µm (Xia & Whitesides, 1998).

The principle of this technique is based on self-assembly and replica moulding, providing the access to 3D structures. For this to be a successful method, it must have a high-resolution photomask to generate the master by photolithography – which is the limiting factor of this process –, with a resolution of 0.8 µm.

After the production of the structure in PDMS, it is necessary to seal it to control the flow of a liquid. This final step can be done with two different approaches: irreversibly and reversibly. To seal irreversibly, both surfaces must be Si-based. An example of a PDMS irreversible bonding is the exposure to an air plasma generating silanol groups (Si-OH) by oxidation of methyl groups and the polymer can seal itself, with glass, silicon or other similar surfaces. On the other hand, PDMS reversible bonding occurs by van der Waals forces (Sia & Whitesides, 2003). Another good method to seal PDMS is the partial curing where some concerns must be taken into account for a successful bonding, like the cleanliness of the surfaces, the ratio of PDMS base to cross-linking agent and the curing process.

This type of devices enriches biological samples analysis and manipulation, since with them there is a substantial reduction of the sample size necessary to do a successful study. Besides this, microfluidic devices can increase reaction rates, improve detection sensitivity and control of adverse events. Despite these benefits, there are some limitations and problems that need to be noted: difficulties in microfluidic connections, the laminar flows inside the device, large capillary forces, clogging, possible evaporation and drying up the sample (Jain, 2008).

1.3.1 Gradient Generator

Adenosine can be found in all cells, which was a concern during the development of this work. An idea of signal for approximately concentrations of adenosine, seems to be a good starting point. To create a system with different concentrations of adenosine which can be measured simultaneously, a miniaturized gradient seems to be a good approach.

Gradients in the properties of surfaces and solutions assume an important role in many biological and chemical processes (Jeon, et al., 2000). It is a process that requires a high degree of control over the position of the individual sources, as well as the quantity of substances they release; conventional techniques lack the appropriate accuracy and stability (Dertinger, Chiu, Jeon, & Whitesides, 2001). To achieve a good gradient, a microfluidic approach can be used, i.e. a Gradient Generator (Figure 1.12), which is the microfluidic device that will have the most emphasis throughout this study. This device has particular characteristics, since it allows the generation of spatially and temporally constant gradients extending over hundreds of micrometers and the maintenance of their shapes over long periods of time (Dertinger, Chiu, Jeon, & Whitesides, 2001). Note that, in order to maintain the shape of the gradient, it is important to reach a steady state, which is easily achieved given the continuous movement of solution along the structure. Since the flow in the microchannels is laminar, the mixing of solutions is done by diffusion at the interface.

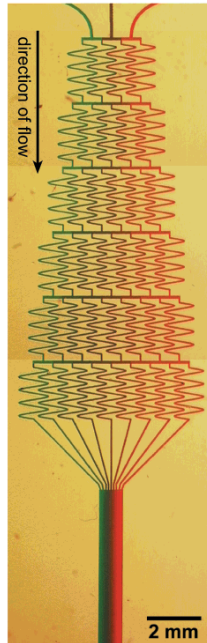


Figure 1.12. Gradient Generator (Dertinger, Chiu, Jeon, & Whitesides, 2001).

As for the structure of the Gradient Generator, it is divided in branches containing an increased number of serpentine until the outlet. When a serpentine of a branch splits to originate two new serpentine of the branch above, the fluid concentration is divided in a way that depends on the splitting ratio for that level (Figure 1.13). All the serpentine have the same length, dimension and resistivity of fluid. It is important to note that the length of the serpentine guarantees a complete diffusive mixing.

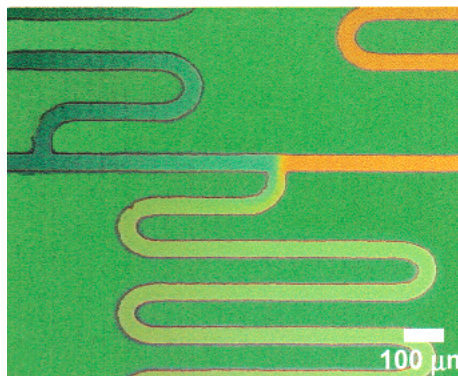


Figure 1.13. Junction of two serpentine with different colours brought together. The colour of the mixed channel was rapidly homogenized (Jeon, et al., 2000).

Besides the Linear Gradient, which represents a good approximation of *in vivo* gradients, it is also possible to create dynamic gradients by varying the relative flow velocities of the input streams of fluids, with a spatial resolution in the order of several microns (Jeon, et al., 2000).

It is important to understand how the mixings occur and what is expected on each chamber. In fact, it is possible to estimate the concentrations achieved at the end of each level of the gradient generator area and consequently the concentrations of each chamber. To estimate these values, some assumptions are made:

- Since the flow is laminar, it is assumed that the mixing is complete;
- When the flow achieves the end of a serpentine channel, the amount of liquid that goes to the right side of the channel is different from the one that goes to the left.

With these assumptions, these calculations can be made in the branching points which are illustrated in the Figure below.

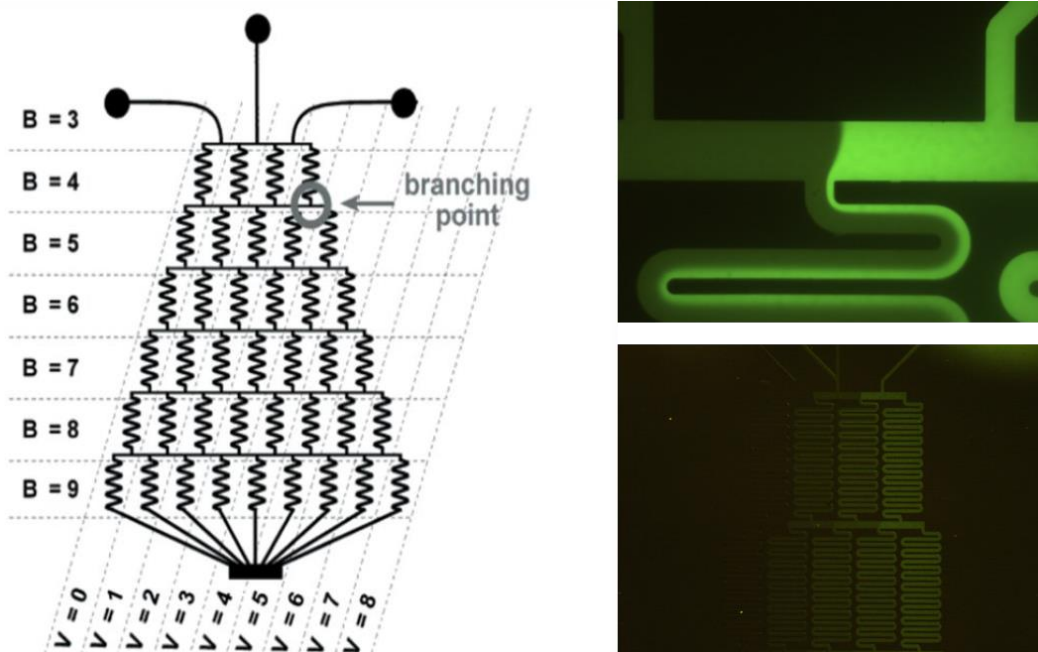


Figure 1.14. Schematic Representation of Gradient Generator and Examples of the Gradient Generator used. In the scheme it is also possible to see how B and V values are distributed.

Firstly, the amount of liquid that flows to each side of the serpentine (left and right side) must be defined:

$$Right\ Side = \frac{V+1}{B+1} \quad (1)$$

$$Left\ side = \frac{B-V}{B+1} \quad (2)$$

Considering three inlets and 6 levels, the splitting ratios were calculated and are represented in Figure 1.15.

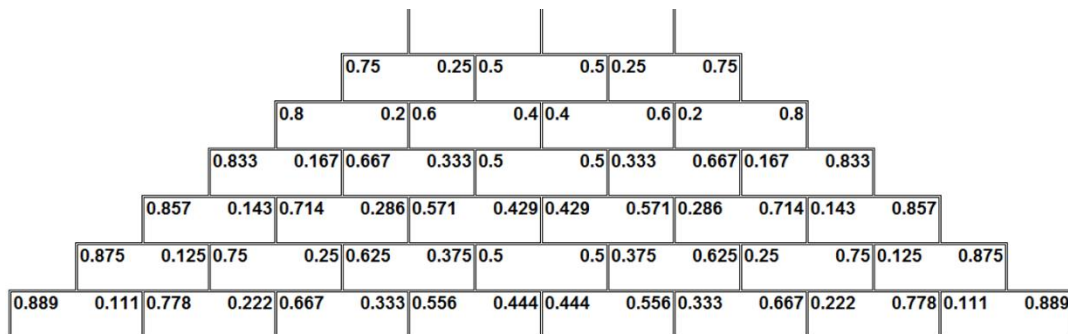


Figure 1.15. Splitting Ratios for a structure with 3 inlets.

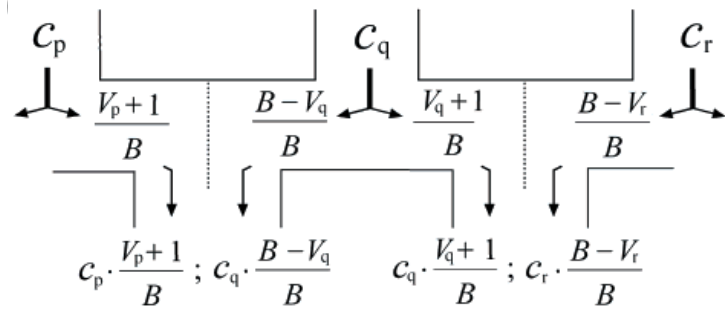


Figure 1.16. Schematic demonstration of calculations in branching points. C_p , C_q and C_r represents the incoming streams. (Dertinger, Chiu, Jeon, & Whitesides, 2001)

Note that the amount of fluid that goes from the extremes to the centre is less each time. Furthermore, in order to obtain the theoretical concentrations of each chamber, it is necessary to multiply the concentration of the incoming streams with the corresponding numbers of the splitting ratio, as illustrated in Figure 1.16.

2 METHODOLOGY

To detect adenosine waves, an aptamer marked with a fluorophore and ssDNA marked with Dabcyl were used, as in (Elowe, et al., 2006).

The two DNA chains are hybridized. In the presence of adenosine, the aptamer bonds with it because it is more stable than bonding with ssDNA. The result is an increase of fluorescence.

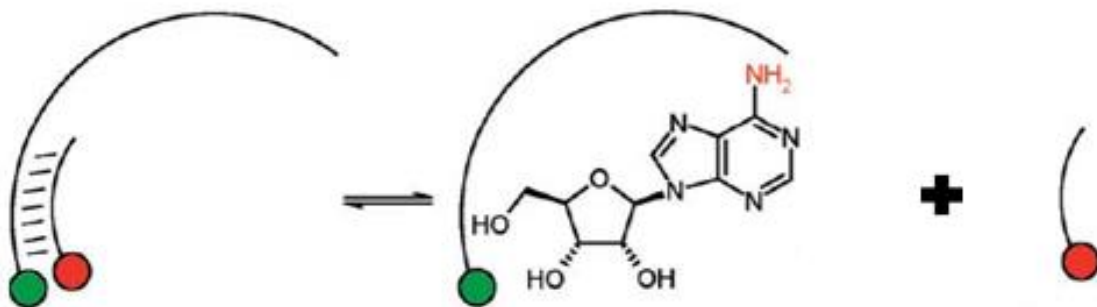


Figure 2.1. Aptasensor for Adenosine. Aptamer for adenosine marked with a Green Fluorophore which is initially bond with a ssDNA-Q with a Dabcyl (red dot) – No fluorescence detected. In the presence of adenosine, the Aptamer is more stable with this molecule and connects with adenosine instead of the ssDNA-Q – the fluorescence increases. (Adapted from (Elowe, et al., 2006))

The aptamer used was: 5'-TCACTG**ACCTGGGGGAGTATTGCGGAGGAAGGT** marked with FAM (Fluorescein amidite) in the 5' extremity (the bold part corresponds to the aptamer for adenosine); from now on, it is designated as Aptamer. It also purchased the ssDNA: 5'-CCCAGGTCAGTG, marked with dabcyl in the 3' end, from now on designed as ssDNA-Q. Both molecules were purchased from *stabvida*. Both stocks of DNA were diluted in Tris-EDTA Buffer (TE),

since with this buffer DNA is soluble and protected from degradation. The TE Buffer was prepared with deionized water and 10 mM Tris and 1 mM EDTA. Both components are from Sigma Aldrich. The equipment and methodology described above was common to all the experiments.

2.1 Macro scale

2.1.1 Quantification of ratio between Aptamer and ssDNA-Q

To understand both the interaction between the aptamer and the ssDNA-Q and the different values of fluorescence involved, a spectrofluorometer was used, in which the excitation and emission wavelengths are set. To perform the measurements, two sets of 6 solutions in eppendorfs of 2 mL were prepared. The first set had 100 nM of Aptamer in all six tubes and different concentrations of quencher in each one: 0 nM, 25 nM, 50 nM, 100 nM, 200 nM and 400 nM. The second set follows the same method but with different concentrations for the aptamer (500 nM) and quencher (0 nM, 125 nM, 250 nM, 500 nM, 1000 nM and 2000 nM). The preparation was as follows: 200 μ L of each solution in a specific order: TE Buffer, Aptamer and ssDNA-Q. To guarantee the bonding between Aptamer and ssDNA-Q, it rested for one hour at room temperature (\sim 20 $^{\circ}$ C). After one hour, the solutions were put in white polystyrene Corning[®] 96 well plates, where the solutions without quencher and another well with TE buffer solutions were the controls.

For the measurements, the spectrofluorometer used was a Varian Cary Eclipse, with the conditions bellow:

- Excitation Wavelength (λ_{ex}): 495 nm
- Emission Wavelength (λ_{em}): 520 nm
- Voltage for the photomultiplier tube: 800V
- Excitation/emission slits: 5 nm

The readings were the average from 5 consecutive measurements with a 0.1 s interval.

2.1.2 Detection of adenosine

Once the ratio of concentrations of Aptamer and ssDNA-Q was defined, adenosine was introduced. A stock of adenosine solution in deionized water with a concentration of 2 mM was prepared. This solution must be heated lightly (not reaching its boiling point) to ensure its homogeneity. The adenosine was purchased from Sigma Aldrich.

The method was similar to the one discussed in 2.1.1., but with fixed concentrations of aptamer and ssDNA-Q, and different concentrations of adenosine.

In these experiments, two different buffers were tested: the same used in (Elowe, et al., 2006), from now on designated as HEPES Buffer, and another used for astrocytes culture (Diógenes, et al., 2014), from now on designated as Astrocytes Buffer.

THE HEPES Buffer was prepared with Milli-Q water and 5 mM $MgCl_2$, 300 mM NaCl and 25 mM HEPES (4-(2-hydroxyethyl)-1-piperazineethanesulfonic acid).

Astrocytes Buffer was also prepared with Milli-Q water and is composed by: 125 mM NaCl, 3 mM KCl, 1.25 mM NaH₂PO₄, 2 mM MgSO₄, 2 mM CaCl₂, 10 mM D(+)-glucose and 10 mM HEPES. All the components of the buffer were kindly provided by IMM: a five times concentrated solution with NaCl, KCl, NaH₂PO₄, D(+)-glucose and HEPES. To prepare a 50 mL Solution, 10 mL of the concentrated solution, 40 mL of Mili-Q water, 100 µL of CaCl₂ and 100 µL of MgSO₄ were used. The pH solution was adjusted to 7.4 with 0.1 M NaOH solution.

To ensure that the binding between Aptamer and ssDNA-Q worked in both buffers, this experiment was performed in the same conditions as the ones previously described.

A set of solutions with a total volume of 200 µL, in 1.5 or 2 mL eppendorfs with different concentrations of adenosine was prepared once more. The conditions of acquisition were the same stated in 2.1.1.

2.2 Micro scale

2.2.1 Gradient Generator

To perform the microfluidic tests, a Gradient Generator (GG) was chosen (described in Section 1.3.1). The microfabrication process was simplified, with the mould kindly provided by Andreia Gameiro (Gameiro, 2013) and it was ready for the soft-lithography.

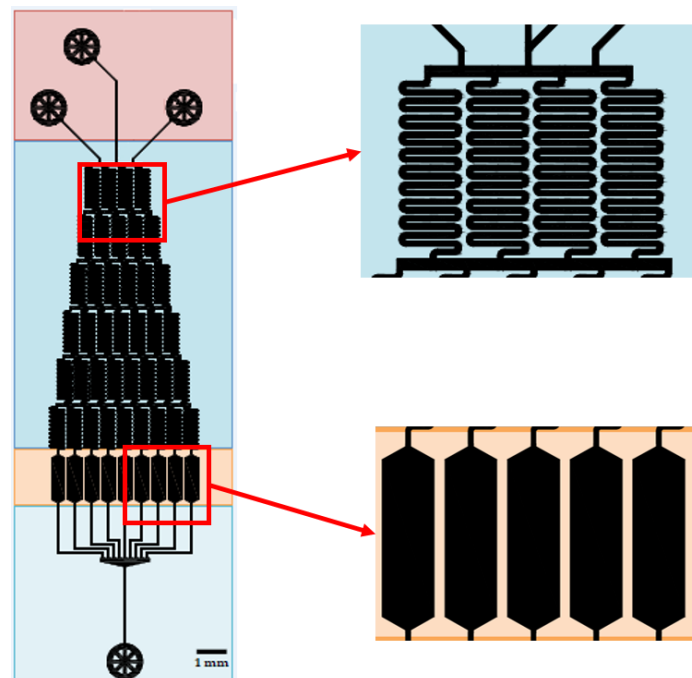


Figure 2.2. Gradient Generator scheme, with detail of serpentine where the mixes occur and the chambers. (Adapted from (Fernandes, Gameiro, Tenreiro, Chu, & Outeiro, 2013))

To obtain the microfluidic device, two dilutions of PDMS and a cure agent were prepared:

- 10:1 (PDMS : Cure Agent) for the device
- 20:1 (PDMS : Cure Agent) for coating a slice of glass for the base of the device

After mixing, these were placed in the degasser for approximately 40 minutes to remove air bubbles.

Then, the 10:1 solution was poured in the mould (which was previously attached to a Petri dish with clean room tape) (Figure 2.3) and the 20:1 was used for coating the glass, using a spinner for 32 s, at a velocity of 2800 rpm and acceleration of 2000 rpm.s⁻¹. Both mould and glass remained in the oven at 70 °C for 50 and 40 min respectively – half cure process.

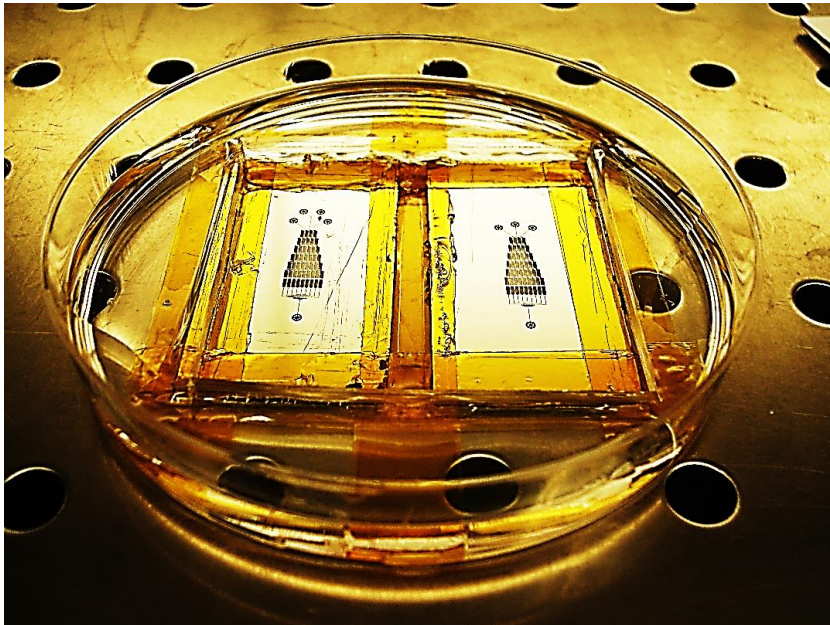


Figure 2.3. Moulds on a Petri Dish, ready to pour PDMS.

Then, both parts (PDMS with the structure and Glass) were joined together and placed again in the oven for 15h. This step allows an irreversible adhesion and completion of the baking process. The final step is to place the inlets and outlet connectors, seal them again with a bit of PDMS mixture and place them in the oven at 70 °C for 1 h. In Figure 2.4, is a picture of a PDMS device ready to use, compared with a 0.01 € coin, to show small the serpentines are.

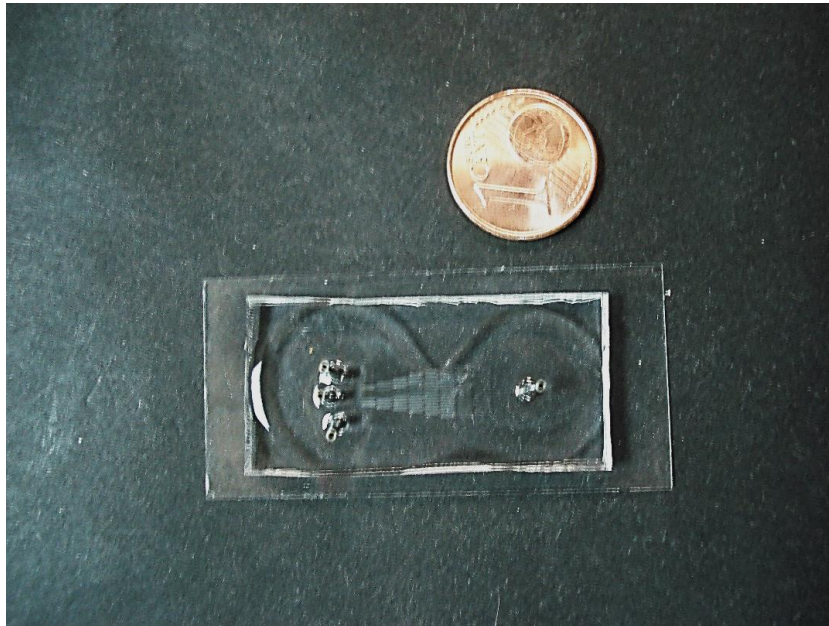


Figure 2.4. PDMS device ready to use.

2.2.2 Tests in the Gradient Generator with Aptamer and ssDNA-Q

Before introducing the adenosine, it is important to verify if the Aptamer and the ssDNA-Q work properly in the microfluidic device. The first test consists of preparing three solutions with a total volume of 100 μL with the same concentrations of Aptamer (500 nM) and with three different concentrations of ssDNA-Q (0 nM, 1000 nM and 2000 nM). The presence (or not) of the ssDNA-Q will result in a gradient at the end of the structure. Before introducing the solutions and because PDMS is hydrophobic, the device was functionalized with Bovine Serum Albumin (1%) (BSA-1%) which was previously prepared with PBS (0.01 M). The BSA molecules are adsorbed by the PDMS and block the device walls (Toepkea & Beebe, 2006). This way, it is guaranteed that the chemical solution with aptamer and quencher will not be adsorbed by the device walls and that it will reach the end of the device with the initial concentrations.

Three syringes were filled with BSA-1% and each one was placed in a syringe pump (Figure 2.5). The connection with the device is made by capillary tube and metallic adapters. The liquid had a flow rate of 2 μL per minute ($\mu\text{L}/\text{min}$) and it flows for approximately 15min. After this, BSA will remain inside the device for a further 10min.



Figure 2.5. Syringe pump during the process of functionalization of the PDMS device with BSA-1%.

After the functionalization, the solutions of Aptamer and ssDNA-Q can be introduced in the device. Because a small quantity of solution is used, it does not fill up the syringe. Each syringe and the capillary tube coupled to it were filled with water; then, the water was slightly pulled back to create a small air space, and the solution was also pulled to the capillary tube. This way, it was possible to have a small air space between water and solution. Each syringe was again placed in a syringe pump (in order to guarantee that all three inlets have the same velocity and to have a linear gradient) and the capillary tube was connected to each inlet through the metallic adapters already inserted in the device, with the specific order shown in Figure 2.6.

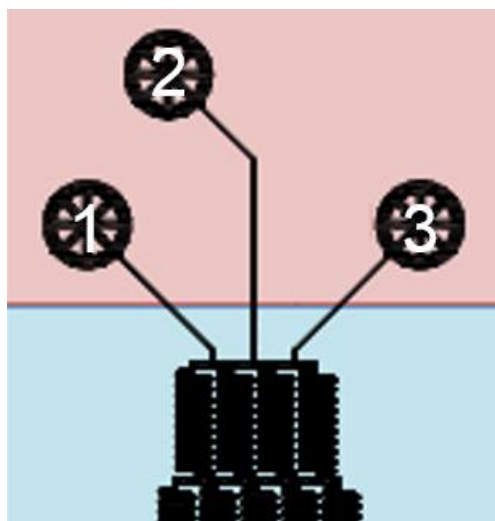


Figure 2.6. Inlets of the Gradient Generator. Inlet 1 corresponds to the solution with 500 nM Aptamer, Inlet 2 corresponds to the solution with 500 nM Aptamer and 1000 nM ssDNA-Q and Inlet 3 corresponds to 500 nM Aptamer and 2000 nM ssDNA-Q.

Each syringe pump was settled with a flow rate of 1 $\mu\text{L}/\text{min}$, and the solutions started to flow into the device. After 15 minutes of flow, the acquisition of images started, in order to verify the stability of the gradient with 1s of exposure time and 2x gain. After the gradient stabilized, the final images were acquired in the same conditions. A picture was taken with each camera, corresponding to a different concentration of quencher. The average fluorescence intensity in the acquired images was measured using ImageJ software. The syringe pumps used were New Era NE300. The capillary tube (BTPE-60) and the metallic adapters were purchased from Instech Solomon and the syringes from Codan. For the image acquisition, a digital camera (DFC300FX) coupled to a Leica DMLM microscope with the light source of a 100W mercury lamp was used. For the excitation of the molecules, a blue excitation light with a band pass illumination path at wavelengths between 450 nm and 490 nm and a long pass observation path above 515 nm was used.

2.2.3 Tests with adenosine using a Microfluidic Structure

The tests with adenosine were performed under similar conditions as the ones described in 2.2.2. Several tests were made and for each one, three solutions with Astrocytes Buffer, 500 nM of Aptamer, 1000 nM of ssDNA-Q and different concentrations of Adenosine were prepared. The first test was made with 0 μM , 500 μM and 1000 μM of Adenosine, and this was the test with highest concentrations performed. The second test had 0 μM , 250 μM and 500 μM of Adenosine and the third test 0 μM , 125 μM and 250 μM .

Once again, the solutions were placed in the Gradient Generator in a specific order:

- Inlet 1 with solution 1 (500 nM Aptamer+1000 nM ssDNA-Q and 0 μM Adenosine)
- Inlet 2 with solution 2 (500 nM Aptamer+1000 nM ssDNA-Q and 50% of maximum concentration of Adenosine in the system – 125 μM)
- Inlet 3 with solution 3 (500 nM Aptamer+1000 nM ssDNA-Q and 100% of maximum concentration of Adenosine in the system – 250 μM)

Before the test, the Gradient Generator was functionalized with BSA (1%) under the conditions described above. After the functionalization, the flow of the solutions and the image acquisition process were also performed in the same conditions as described above. The same materials were used as well as the programme to measure the average fluorescence.



Figure 2.7. Setup of the Experiments using the gradient generator, in the Microscope.

2.2.4 Immobilization of the Aptamer

For the immobilization of the Aptamer at the surface, the experiment chosen was the electrostatic immobilization. For this experiment a straight channel with 20 μm high, 200 μm width and 4 mm length was used.

The method of fabrication for this PDMS device is slight different from the one presented for the gradient generator, since it is not used the process of half-cure.

For the fabrication of this PDMS device, a dilution of PDMS was prepared 10:1 (PDMS: Cure Agent), and poured into the mould attached to a petri dish and went to the oven for 1h at 70°C. After taking the PDMS of the mould, the PDMS and a piece of glass were placed in UVO for 15 minutes. Then, the PDMS and glass were joined and went again to the oven at 70°C for at least 4h.

With the straight channels ready, the next step is to prepare the surface of the channels for the immobilization. The first step is to treat the channel with Corona, creating small impulses of 1s inside the channel. Next, an APTES (2%) solution was prepared with 200 μL of Ethanol and 5 μL of APTES (96%) and flowed to the channel for 10 minutes with a flow rate of 1 $\mu\text{L}/\text{min}$ and 5 minutes more without flow, just the liquid inside. The materials used such as syringe pump, syringes and capillary tube are the same already mentioned. Next, the APTES must be washed from the channel and this is done in two steps: Ethanol and deionized water. First Ethanol is flowed for 5 minutes with a flow rate of 5 $\mu\text{L}/\text{min}$ and stays inside the channels for 5 minutes more, then the same procedure is applied for the deionized water.

The next step is to flow the Aptamer into the channel and for that purpose a solution with a concentration of 5 μM was prepared with Astrocytes Buffer for a total volume of 20 μL . Since this small amount of solution is not enough to fill up a syringe, the syringe and capillary tube coupled to it were

filled with water and slightly pulled back to create a small air space, and then the solution was also pulled into the capillary tube. For 10 minutes, with a flow rate of 1 $\mu\text{L}/\text{min}$ the solution of aptamer was flowed inside the channel and stayed inside for more 5 minutes. To remove all the molecules that did not bind to the surface, the channel was washed with Astrocytes Buffer for 5 minutes with a flow rate of 2 $\mu\text{L}/\text{min}$. To verify if the Aptamer bound to the surface, the channel was measured in an inverted microscope with acquisition conditions of 2s Exposure and 5 dB of Gain. The microscope used was Olympus CKX-41, with a digital camera (Olympus XC30) coupled to acquire images. Then, a second molecule was added to the channel: ssDNA-Q. A solution with total volume of 20 μL was prepared with Astrocytes Buffer and ssDNA-Q concentration of 10 μM , and was placed in the capillary tube with the same technique creating a bubble air between water and solution. The method for the flow the solution with ssDNA-Q to the channel was the same used for the Aptamer (10 minutes with 1 $\mu\text{L}/\text{min}$ flow and 5 more minutes without flow), just like with Astrocytes Buffer. After the wash, the channel was measured again with the same conditions.

Last step was the introduction of adenosine, a solution with 5 mL of total volume and 500 μM of adenosine with a flow rate 0.5 $\mu\text{L}/\text{min}$. In this last step, the acquisition of images was taken in intervals of 20 seconds, and in the same conditions already explained.

3 RESULTS AND DISCUSSION

On this chapter, besides showing the main results of this work, a brief analysis will be done. This analysis will be divided into four main sections.

On the first section, the interaction of the Aptamer and ssDNA-Q will be discussed, as well as a comparison of the fluorescence of the aptamer, in the presence of different buffers. In this section, the tests were done by preparing solutions with the same concentration of aptamer and different concentrations of ssDNA-Q, in three different buffers. Then, to measure the different fluorescence signals, a spectrofluorometer was used. In this section the ideal ratio between Aptamer and ssDNA-Q was settled in order to quench the fluorescence signal enough as well as a prediction of which buffer will work better in the presence of adenosine.

In the second section, adenosine was introduced in the system. On this set of experiments, the concentration for Aptamer and ssDNA-Q was constant and different concentrations of adenosine were settled in the preparation of the solutions, using different buffers. Again, the solutions were measured in a spectrofluorometer. Furthermore, in this set of experiments, the main purpose was to understand the behaviour of the adenosine with the mix Aptamer+ssDNA-Q in different buffers.

With the knowledge of the two previous sections, a miniaturized system was chosen. On the third section, some first tests will be done with the chosen microfluidic device, the gradient generator. The focus of this section will be its proper functionalization, which is performed with BSA (1%), as well as the behaviour of Aptamer, ssDNA-Q and adenosine. The main results presented on this section are based on two different experiments. One, with a constant concentration of Aptamer and different

concentrations of ssDNA-Q and another experiment with constant concentrations of Aptamer and ssDNA-Q and different concentrations of adenosine.

With the proper functioning, between the microfluidic device and the molecules of interest, proved in the previous section, the fourth section will expose all the results related to the efforts to optimize this system in order to achieve the adequate concentrations of adenosine. Additionally, this section besides the work developed to optimize the system with the gradient generator, the possibility of immobilizing the aptamer will also be discussed.

3.1 Molecular Interaction between ssDNA-Q and Aptamer

The first step of this experimental work was to ensure a proper interaction between Aptamer and ssDNA-Q. For this first experiments, the spectrofluorometer with the conditions already explained in previous section was used. This step of the work is crucial, since it is necessary to guarantee that the binding between the Aptamer and ssDNA-Q significantly reduces the signal because of the quenching. This way, it will be possible to see an increase of fluorescence in the presence of adenosine, since the system is more stable with the Aptamer rather than with ssDNA-Q.

Although it was not a main part of the work, experiments in spectrofluorometer with the same concentrations of Aptamer and ssDNA-Q but different buffers revealed to have dissimilar results. It is important to note that these dissimilar results are related to the intensity of the signal and not the interaction between Aptamer and ssDNA-Q, as will be presented. Since the type of Buffer influences the behaviour of the system, a study about each of them, seems to be appropriate. In this section, the intensity of the prepared solutions versus the amount of Aptamer and ssDNA-Q will be related and compared for the different buffers used. All the results presented on this section were performed on the Spectrofluorometer, using a 96 well-plate.

3.1.1 Tris-EDTA (TE) Buffer

The first buffer used to test the interaction between the Aptamer and ssDNA-Q was the same as the one used to dilute the molecules. As mentioned before, the choice of this buffer for dilution is obvious, as it is a common buffer in molecular biology and its properties prevent the degradation of DNA. Based on these facts, the first set of tests was undertaken, towards an ideal concentration of Aptamer and ssDNA-Q. To understand the amount of molecules needed to produce a good fluorescence of aptamer, two different concentrations of aptamer and respective ratio of ssDNA-Q were used. The results are represented Figure 3.1.

In both cases, the effect produced by ssDNA-Q was a decrease of the fluorescence, more relevant for higher concentrations of ssDNA-Q.

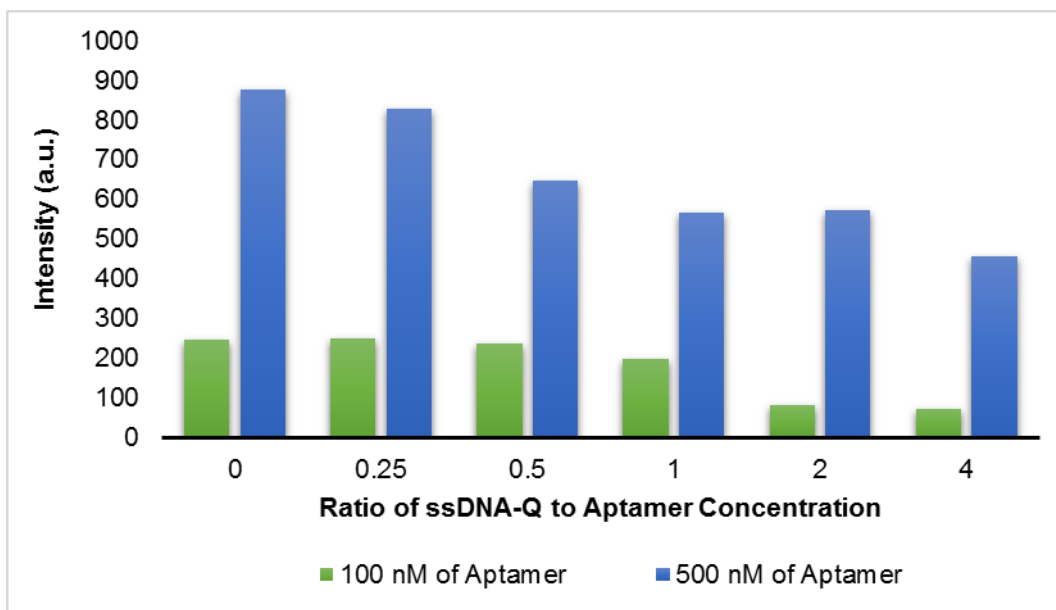


Figure 3.1. Comparison of Fluorescence between different concentrations of Aptamer and ssDNA-Q, using TE Buffer.

After this first test, the focus of the study was directed to higher concentrations of aptamer and the relation with ssDNA-Q. A new experiment was performed, but with higher concentrations of ssDNA-Q than the one before.

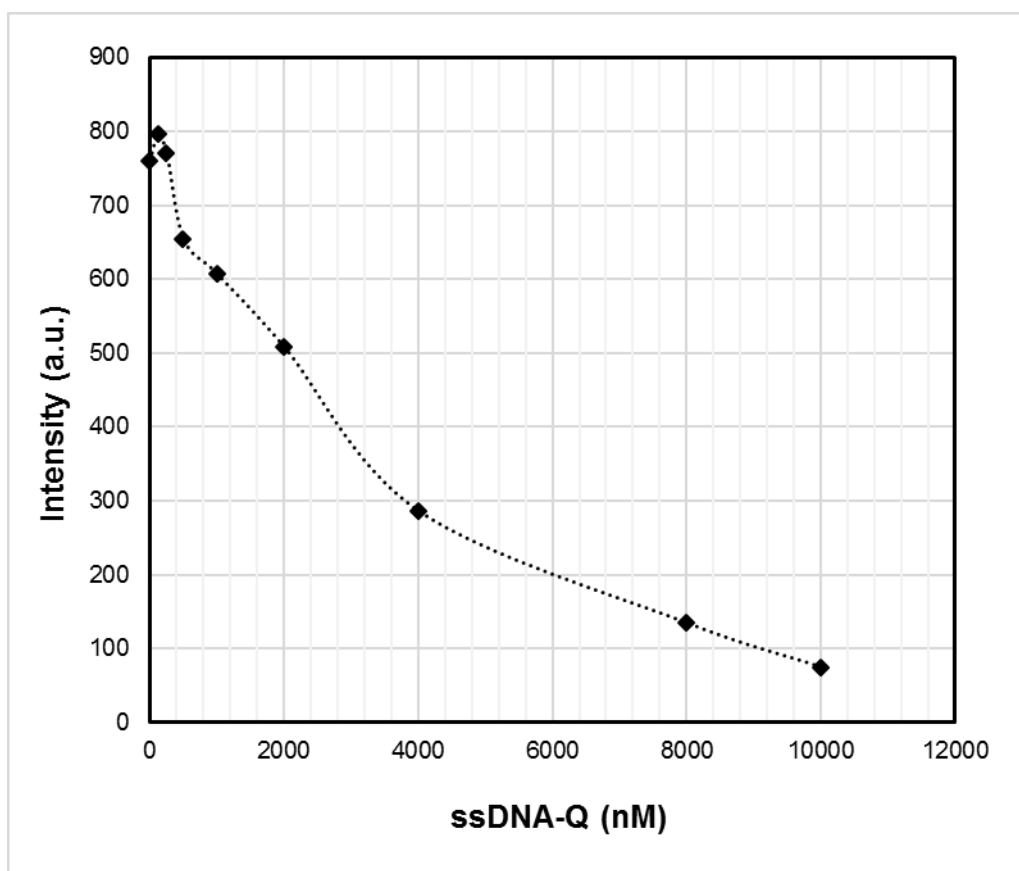


Figure 3.2. Fluorescence intensity of 500 nM Aptamer with different concentrations of ssDNA-Q, using TE-Buffer.

3.1.2 HEPES Buffer

Although the TE Buffer seems to work properly for the interaction between the Aptamer and ssDNA-Q, there are some concerns about its influence in the proper conformation of the Aptamer, and consequently, proper binding to the adenosine. With this concern in mind, for the next experiment, the buffer chosen was the same that (Elowe, et al., 2006) used for the same Aptamer and ssDNA-Q. This buffer is constituted by 5 mM MgCl₂, 300 mM NaCl and 25 mM HEPES at pH 8.0.

Again, the behaviour of ssDNA-Q is more evident due to its higher concentrations (Figure 3.3). Comparing with the TE Buffer, the curves are similar, under the same conditions but with different orders of magnitude:

- For TE Buffer, the intensity of 500 nM Aptamer without ssDNA-Q is 761 a.u. ± 3
- For HEPES Buffer, the intensity of 500 nM Aptamer without is 75.5 a.u. ± 0.3

This decrease in Fluorescence can be explained by the components of the HEPES Buffer, in particular the NaCl and MgCl₂ due to the interaction of the cations Na⁺ and Mg²⁺ and the fluorophore present in the Aptamer (FAM). In fact, as (Juskowiak, Galezowska, Zawadzka, Gluszynska, & Takenaka, 2006) describes, fluorescence intensity of FAM is sensitive to the nature and concentration of cations. In fact, it is described that some cations such as Li⁺, Na⁺, K⁺ and Mg²⁺ causes quenching in the FAM fluorescence. Furthermore, the authors say that the concentrations of cations required for 50% quenching of FAM fluorescence were estimated as follows: 2 μM of K⁺, 1 mM of Mg²⁺, 20 mM of Na⁺ and 80 mM of Li⁺ (Juskowiak, Galezowska, Zawadzka, Gluszynska, & Takenaka, 2006). Comparing with the concentrations of Na⁺ (300 mM) and Mg²⁺ (5 mM) present in the HEPES Buffer, the decrease of fluorescence is justified.

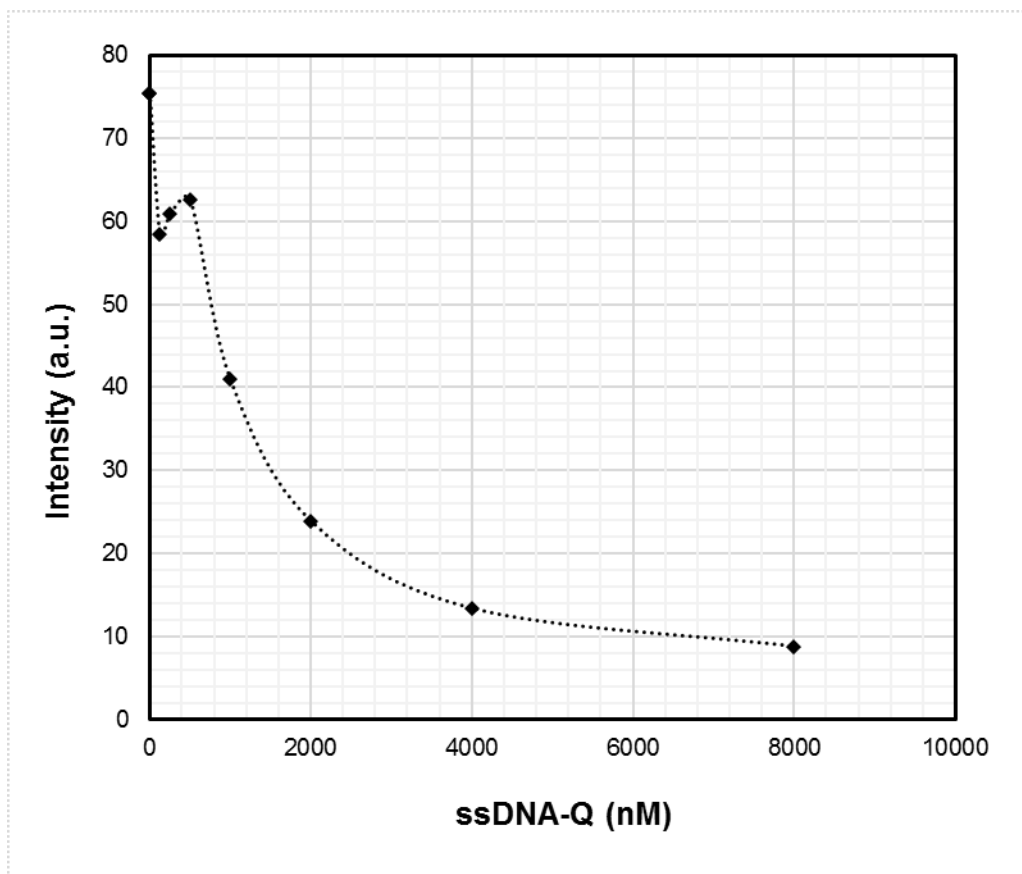


Figure 3.3. Fluorescence intensity of 500 nM Aptamer with different concentrations of ssDNA-Q, using HEPES Buffer.

3.1.3 Astrocytes Buffer

Despite the HEPES Buffer, as stated in (Elowe, et al., 2006) working properly in the interaction of the three molecules, the low signal presented in the previous section may be a concern when proceeding to the miniaturization of the system. Another concern, for a future perspective, is the behaviour of the Aptamer and ssDNA-Q in cells.

With these issues, a third Buffer was tested to see how sensitive the binding between Aptamer and ssDNA-Q was with a more complex buffer in terms of components. The buffer chosen is used for fluorescence measurements in astrocytes. There are two components of this buffer similar to HEPES Buffer: NaCl (but with a much lower concentration) and HEPES. Furthermore, pH of Astrocytes Buffer is slightly different (pH=7.4) which also may be a critical point. With these concerns, the experiment was performed and the result is illustrated in Figure 3.4.

The Aptamer and ssDNA-Q, have a good binding again, since the fluorescence decreases with ssDNA-Q. The effect of ssDNA-Q is clearer to higher concentrations. Comparing the three buffers, TE Buffer is the one that presents a major intensity for 500 nM of Aptamer without ssDNA-Q (761 a.u. \pm 3) followed by Astrocytes Buffer (391 a.u. \pm 2) and HEPES Buffer presents the lowest signal (75.5 a.u. \pm

0.3). As already explained in the previous section, the fluorescence for the same concentration of Aptamer is due the presence of cations. In the case of Astrocytes Buffer, the influence of the cations is not as dramatic as in HEPES Buffer. A brief analysis of the cations present on this Buffer can explain this. Analysing the concentrations of each component of the Astrocytes Buffer, the cations concentrations are: 126.25 mM Na⁺, 3 mM K⁺, 2 mM Ca²⁺ and 2 mM Mg²⁺ and comparing with the ones estimated by (Juskowiak, Galezowska, Zawadzka, Gluszynska, & Takenaka, 2006) required for 50% quenching of FAM, the difference between TE Buffer and Astrocytes Buffer is explained. Furthermore, the signal difference between Astrocytes Buffer and HEPES Buffer can be explained by the different pH of each buffer, to which the fluorophore is sensitive.

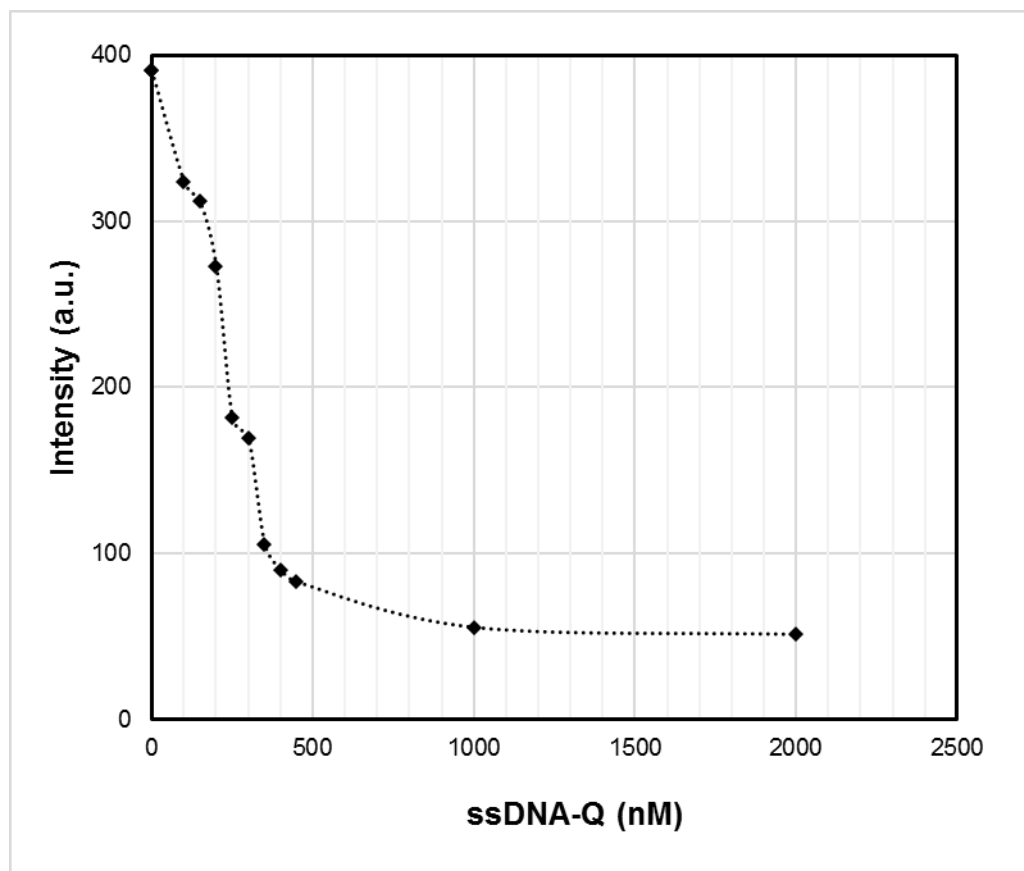


Figure 3.4. Fluorescence intensity of 500 nM Aptamer with different concentrations of ssDNA-Q, using Astrocytes Buffer.

3.1.4 Comparing Intensity of Fluorescence of Aptamer for different Buffers

Although the decrease of fluorescence with ssDNA-Q is clear in all buffers, the intensity is very different, due to the different components of the three buffers. In this section, the three buffers are compared in order to predict the behaviour of the Aptamer and ssDNA-Q in the presence of adenosine.

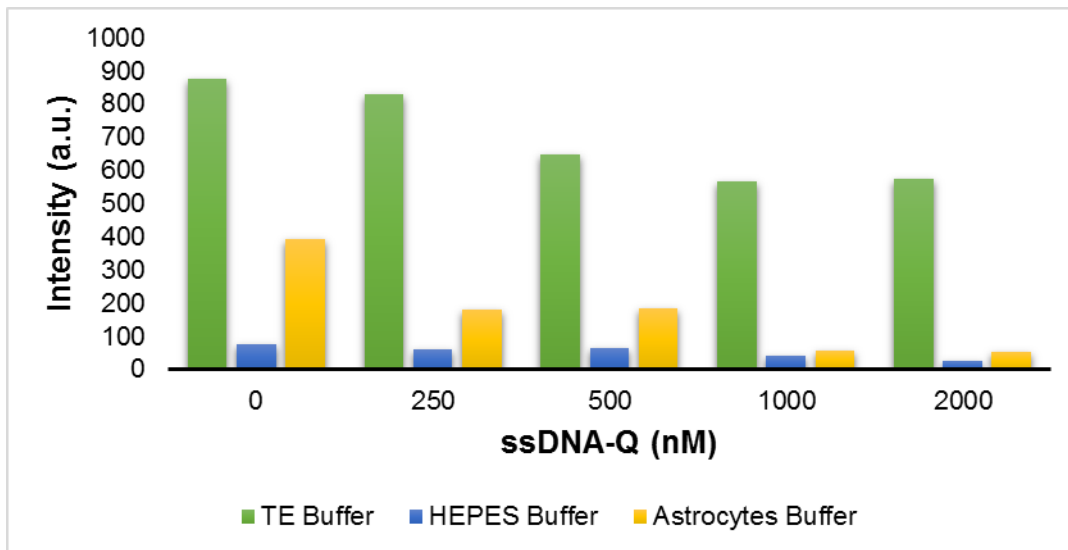


Figure 3.5. Fluorescence Comparison between the three Buffers. (500 nM Aptamer and different concentrations of ssDNA)

It is evident that the best fluorescence is from the TE Buffer, but the absence of some components may compromise the interaction between the Aptamer and adenosine. On the other hand, and with future perspectives of miniaturizing the system, the fluorescence in the presence of HEPES Buffer is very low. This may compromise future experiments in microscale. Although the Astrocytes Buffer seems to be the best option for future experiments, because of its good fluorescence and probably not compromise the interaction between Aptamer and adenosine, in the next experiments with adenosine the three buffers will be used.

3.2 Behaviour of Aptamer and ssDNA-Q in the presence of adenosine

The interaction tests between the Aptamer and ssDNA-Q allowed the definition of their concentrations for the tests with adenosine: 500 nM Aptamer and 1000 nM ssDNA-Q. A test was performed for each Buffer, using different concentrations of adenosine. As already mentioned and expected, it was not possible to detect adenosine with the TE Buffer, since the intensity for different concentrations of adenosine was approximately the same. This result confirms that, although the TE Buffer is a good buffer to store DNA, it interferes with the structure of the Aptamer, which is crucial to bind with Adenosine instead of ssDNA-Q. Additionally, the test performed with the two other Buffers was more successful (Figure 3.6 and Figure 3.7). Again, and as expected, the curve has similar shapes in both Buffers, but different orders of magnitude. The reasons are the same already presented in the previous section.

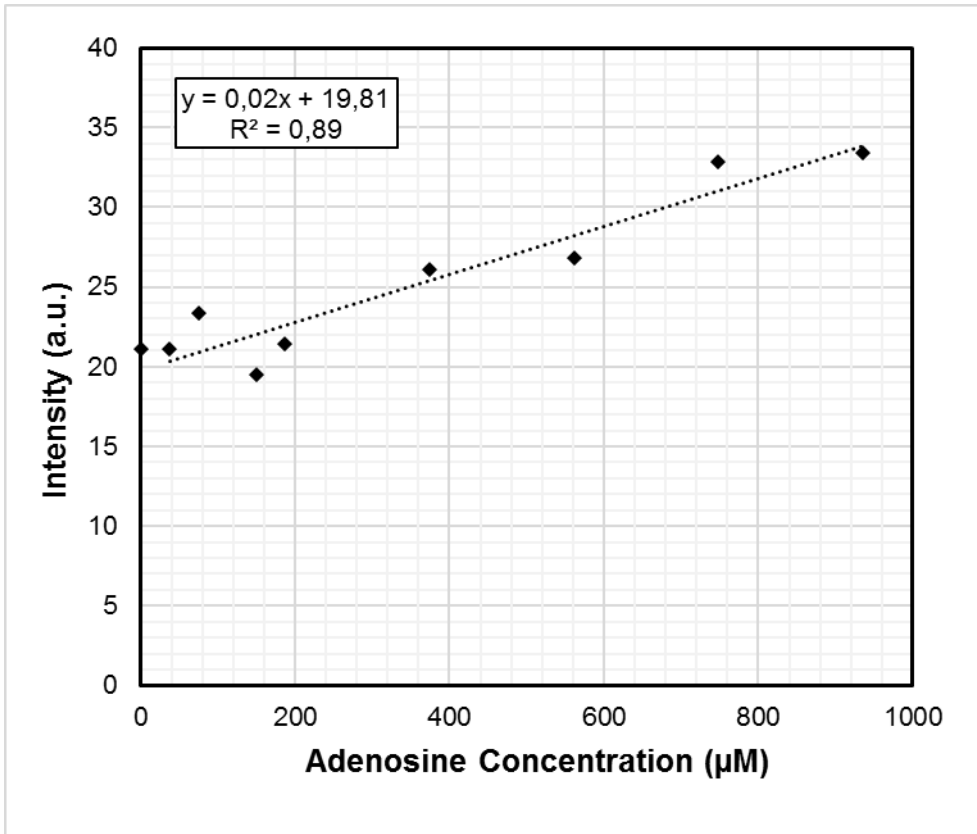


Figure 3.6. Fluorescence intensity of 500 nM Aptamer and 1000 nM ssDNA-Q with different concentrations of Adenosine, using HEPES Buffer.

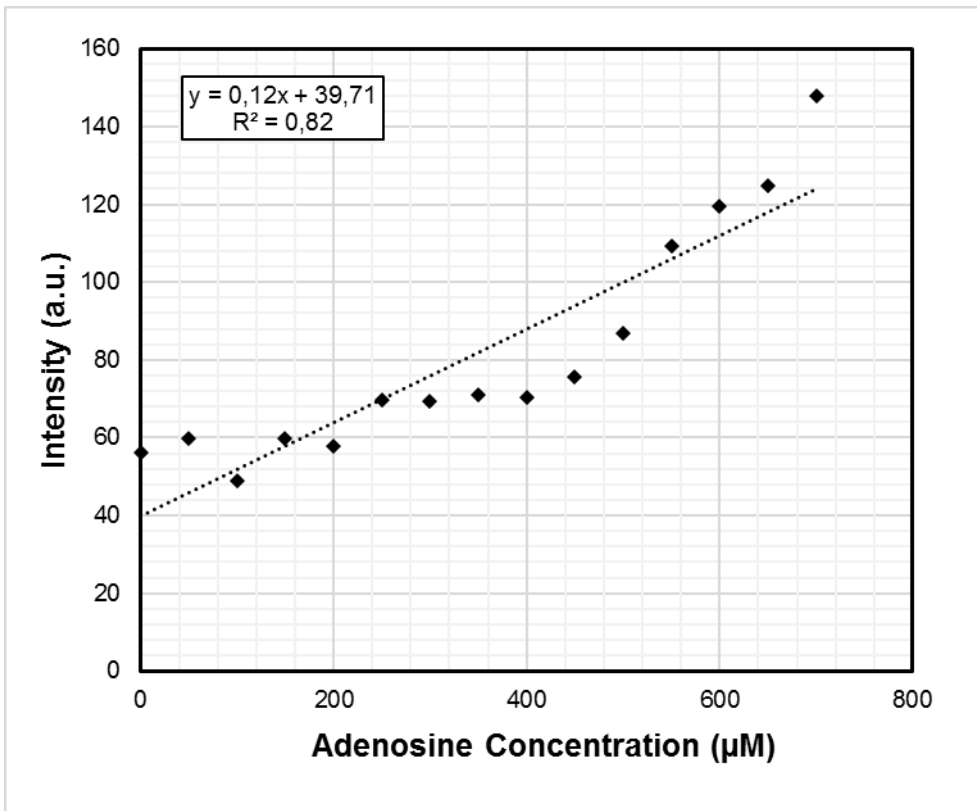


Figure 3.7. Fluorescence intensity of 500 nM Aptamer and 1000 nM ssDNA-Q with different concentrations of Adenosine, using Astrocytes Buffer.

Analysing the graphs, the first concern is the proper fit for the system and the equilibrium between Aptamer-ssDNA-Q and adenosine. In fact, and as reported by (Halperin, Buhot, & Zhulinay, 2005) the hybridization between a probe and a target is normally described by the Langmuir model. Although this method is described for immobilized probes, the behaviour of adenosine illustrated in the graphs allows a qualitative analysis, based on the Langmuir, since this is a model applied to equilibrium states, which is the case. Considering the Aptamer (A) a probe and adenosine (B) a target, they can be described by a hybridization reaction such as:



The equilibrium constant can be calculated:

$$K = \frac{AB}{A \times B} \quad 4)$$

If we add an equation of mass conservation for B, we obtained a graph similar to the presented above.

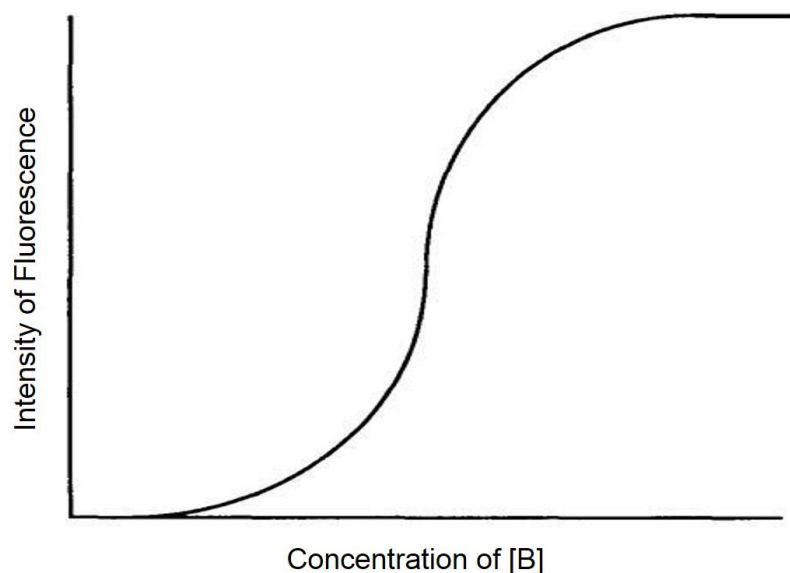


Figure 3.8. Behaviour of Adenosine according to a Langmuir Model

Observing Figure 3.8, it is possible to achieve some interesting points for the analysis of the results of this work. Considering the equilibrium constant (K) and different concentrations of adenosine there are three critical points: when adenosine is far from K (lower or higher), there will be a low increase of fluorescence. Furthermore, for concentrations close to K, there will be a quick increase of fluorescence. Comparing with the results presented, it is a similar behaviour. In order to simplify the analysis of the data and whenever it is necessary, although the behaviour is similar to Langmuir Model, a linear regression will be done as approximation to this model, since the values used seem to be all close to K value.

Another important concept for the correct analysis of the graphs and a proper understanding of the amount of adenosine that can be detected is the Limit of Detection (LoD). The limit of detection

expresses the lowest concentration of analyte that can be detected for a given type of sample, instrument and method. To this particular case, the LoD will be calculated using the regression line for each graph. The LoD is then, calculated from the intercept and standard error of the regression line:

$$c_{LOD} = \frac{s_{y/x}}{b} \times 3.3 \quad (5)$$

Where $s_{y/x}$ represents the standard error of the predicted y-value for each x in the regression and b represents the slope from the equation of the regression line $y = mx + b$ and the number 3.3 is a factor of multiplication.

The LoD for adenosine was then calculated for each Buffer, and the results are below.

	Slope (b)	$S_{y/x}$	LoD for adenosine (μM)
HEPES Buffer	0.01	1.8	584
Astrocytes Buffer	0.12	12.9	354

Figure 3.9. Values for the calculation of Limit of Detection for each Buffer.

Comparing the LoD for adenosine for each buffer, it can be observed that although different, are very high for the main objective of this work. Furthermore, these tests confirmed that the interaction between the three molecules was adequate, although the concentrations of adenosine were not the ones desired. The next step is to optimize the system to detect physiological concentrations of Adenosine (in the order of 20 μM , maximum). Although both buffers seems to not interfere with the functioning of the molecules, as a matter of future work perspectives with astrocytes, from now on all the experiments will be performed with the Astrocytes Buffer.

3.3 The Gradient Generator and the behaviour of Aptamer, ssDNA-Q and Adenosine

Based on the results and analysis made for macro scale, a miniaturized system was used to reproduce similar results in micro scale. Andreia Gameiro's microfluidic device was chosen for this task. This device, as previously explained, is the Gradient Generator.

In this section, all results obtained in the optimization of the Aptamer-ssDNA-Q to detect physiological concentrations of adenosine will be concisely explained. In the first subsection, the functionalization of the microfluidic device and a control test with Aptamer and ssDNA-Q will be present, to allow an understanding of how these work using a Fluorescence Microscope and this specific microfluidic device, instead of a spectrofluorometer and the microplate. The second subsection will show the first results when introducing the adenosine and its behaviour.

Finally, the third subsection will explain the efforts made to optimize the system, in order to detect lower concentrations of adenosine.

3.3.1 Functionalization of the Gradient Generator and Control Test with Aptamer and ssDNA-Q.

The first step was to ensure that the PDMS device is suitable for avoiding non-specific adsorption. The main concerns are:

- If the solutions will maintain their concentrations along the device,
- If the gradient established is linear at the end of the device (as expected).

The first concern arises from the hydrophobicity of PDMS, already explained in Chapter 2, and can compromise the concentrations of solutions along the device. It is then necessary to functionalize the structure, in order to promote the wetting of the PDMS walls. For this functionalization, a Bovine Serum Albumin (BSA) Solution, 1% in PBS, was used. This will result in the BSA molecules being adsorbed by the PDMS walls, to prevent non-specific adsorption.

The second concern arises from a theoretical analysis of the concentration expected in each camera of the gradient generator, and in this specific case, for a linear gradient. The next subsection will discuss this subject and present a test with Fluorescein Isothiocyanate (FITC) to test the device.

After guaranteeing the proper conditions of the PDMS device, the experiments described in Section 2.2.2 were performed. They will be discussed in Section 3.3.1.2.

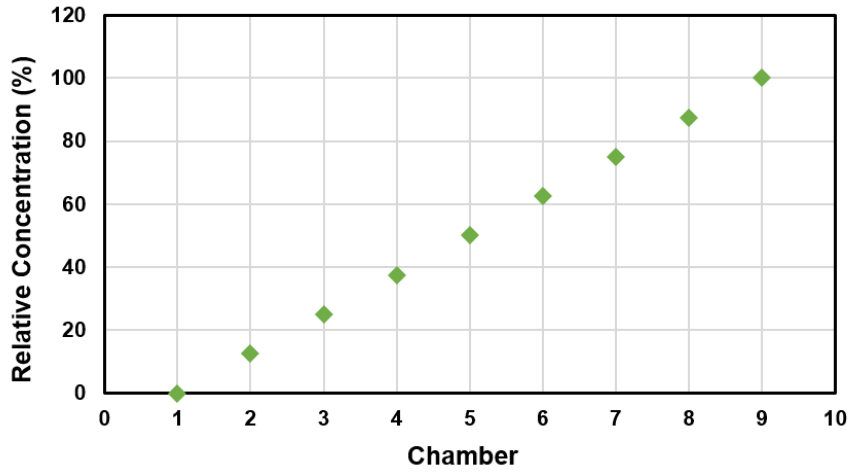
3.3.1.1 The Theoretical Linear Gradient and the FITC Test

The Gradient Generator used for the experiment has four main parts:

- 4 inlets (although one is not used, since it is meant for the introduction of cells which do not have part in these experiments);
- A gradient generator area, composed by 6 levels with serpentine channels, in order to increase the contact area between the chemical solutions introduced;
- 9 chambers corresponding to the final concentrations of the solutions generated;
- One outlet.

As already described in section 1.3.1, it is possible to predict the concentrations of each chamber. In Figure 3.10, the concentration is represented for each corresponding chamber, in a table and graphically. This is a linear gradient, but this type of devices can produce much more than just simple linear gradients. To have another type of gradient, it is necessary to change some parameters, such as the flow rate and the concentrations of the solutions in the inlets.

With all the theoretical values settled, it is time to test the device. Since it is already an optimized device, only a brief test with FITC was performed, with the concentrations 0 $\mu\text{g/mL}$ (inlet 1), 10 $\mu\text{g/mL}$ (inlet 2) and 20 $\mu\text{g/mL}$ (inlet 3), and the acquisition conditions were 250 ms of exposure and 2x gain. As already mentioned, the first step was to functionalize with BSA-1% and then FITC molecules with a flow rate of 1 $\mu\text{L/min}$. After 30 minutes, the gradient stabilized and images were acquired. For the analysis of Fluorescence, ImageJ was used. The results values are illustrated in Figure 3.11.



Chamber	Relative Concentration (%)
1	0
2	12.5
3	25
4	37.5
5	50
6	62.5
7	75
8	87,5
9	100

Figure 3.10. Theoretical Values for each Chamber of the Gradient Generator.

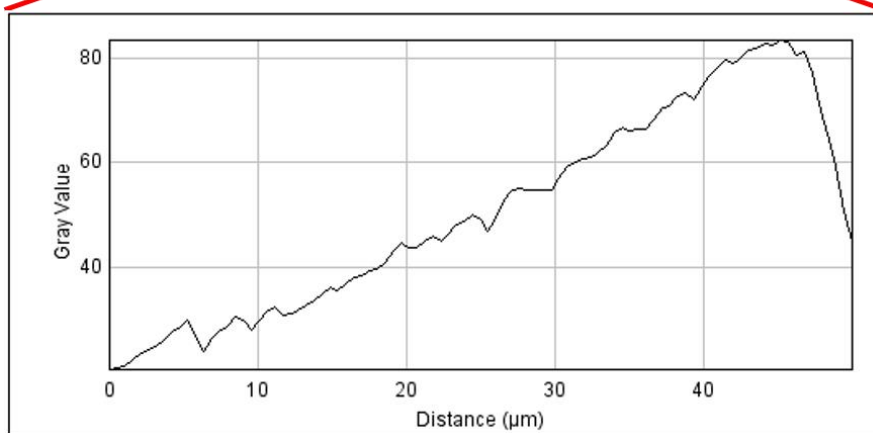
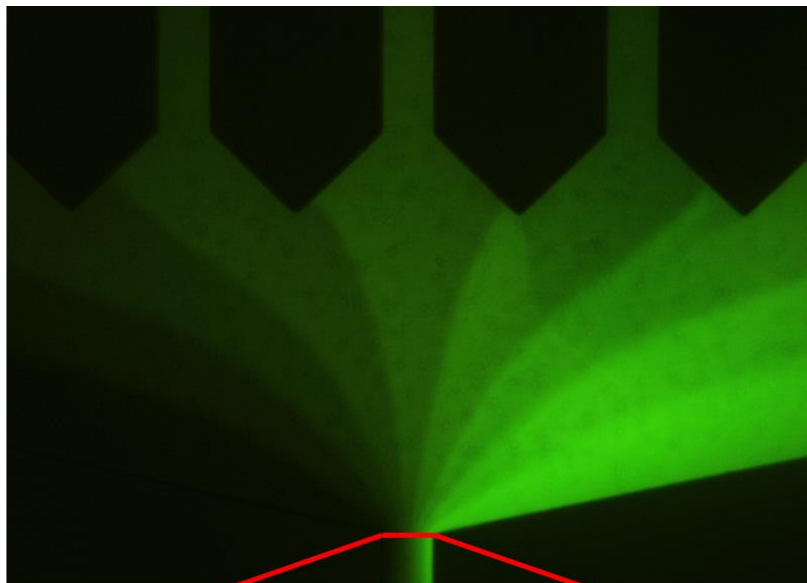


Figure 3.11. Outlet of the Gradient Generator and a Profile Plot from ImageJ.

The profile plot represents the grey values of the outlet, where all the 9 new solutions converge with a laminar flow, as shown in the picture. The behaviour of the profile plot is linear, as predicted theoretically, which confirms that the PDMS device is working properly and the work can proceed with the aptamer and ssDNA-Q.

3.3.1.2 Gradient with Aptamer and ssDNA-Q

Although the good interaction between aptamer and ssDNA-Q was already proven on previous sections, it is necessary to study how they work in this new approach. For that, a few tests were performed, according to the procedures described in Section 2.2.2.

At the start of the image acquisition, the system must be stable. For that reason, the acquisition of images was set to start 20 to 30 minutes after the solutions were flowed into the PDMS device. For these first tests, the conditions of acquisition were 1s Exposure and 2x Gain.

The concentrations of ssDNA-Q for each chamber were calculated based on theoretical values presented in Section 3.3.1.1 and is represented in Figure 3.12.

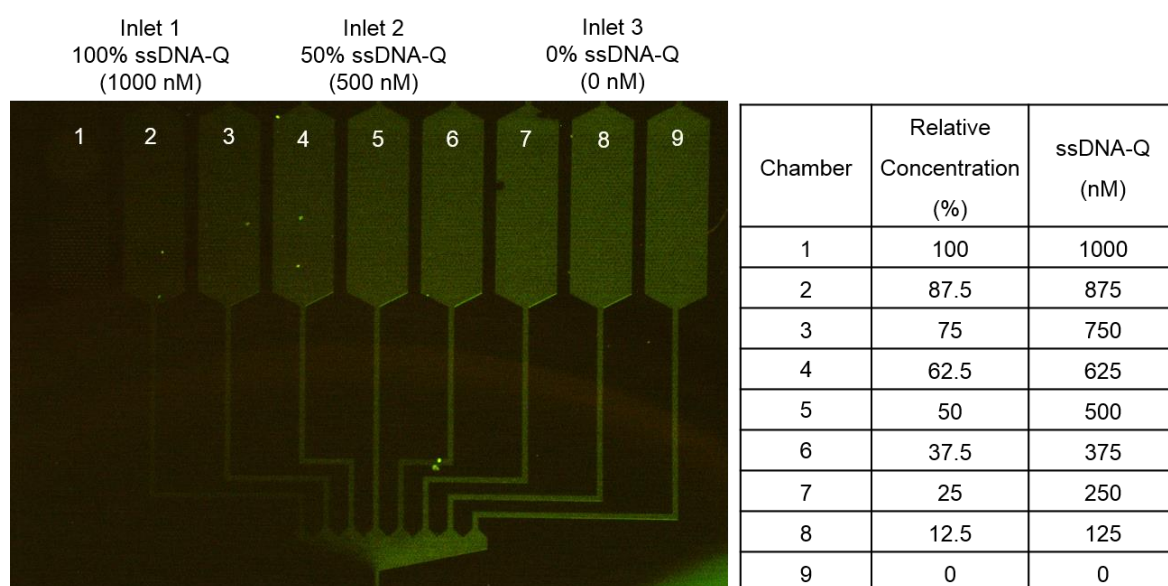


Figure 3.12. Illustrative Picture of the 9 Chambers, concentrations from each inlet and expected values of ssDNA-Q are represented on the table.

Pictures were taken of each chamber and analysed with ImageJ. For each chamber, three different areas of interest were measured and the background was subtracted to each one. The result for each chamber is the average of the three results.

There is an obvious decrease in fluorescence with ssDNA-Q (Figure 3.13). The low values of error for each point are justified by the uniformity of the signal along the chamber. Comparing with the results obtained in macro scale for the same buffer (Astrocytes Buffer) the difference in intensity of fluorescence is evident, although the curves follow a similar behaviour (Figure 3.14). This result is explained by several factors but with main focus for the quantity of molecules that are measured in the different cases (the volume of solution used was much higher in the macro than in the microscale

experiments) and the completely different conditions in both experiments: spectrofluorometer vs microscope; intensity of excitation light and light travel path.

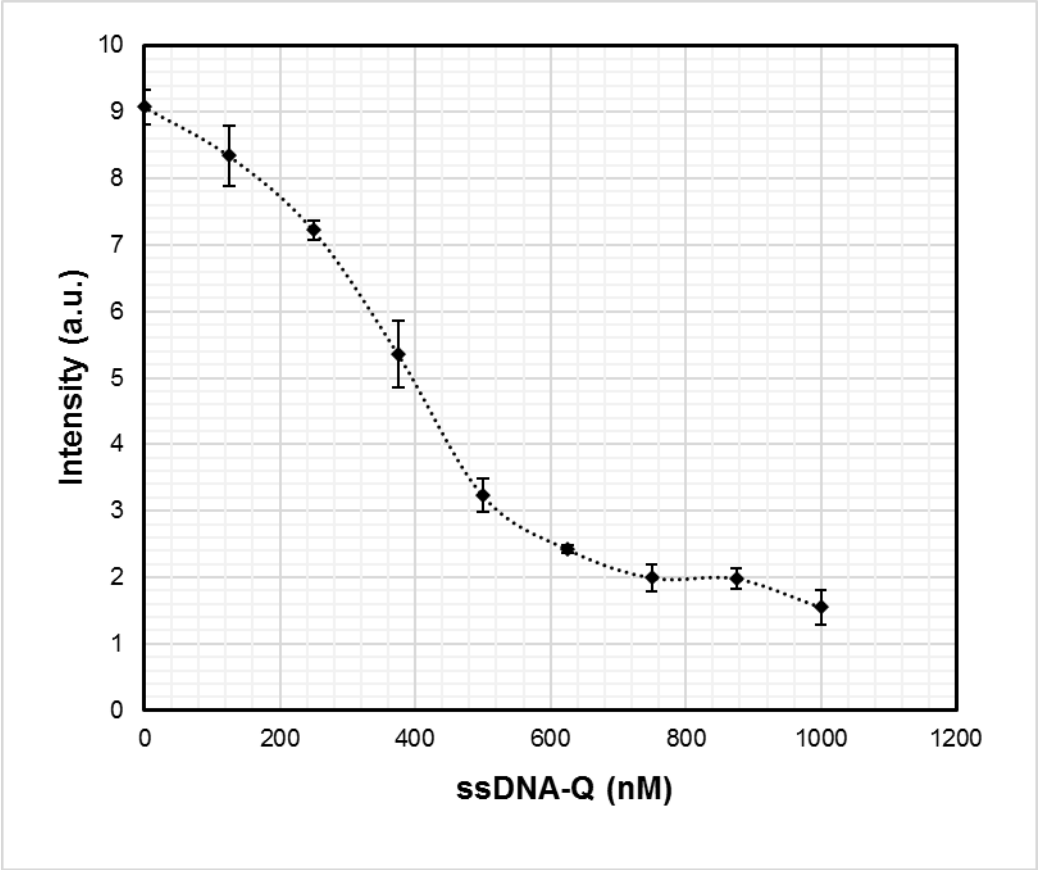


Figure 3.13. Fluorescence Intensity for 500 nM of Aptamer and various concentrations of ssDNA-Q, in PDMS device. Each point represents a different chamber.

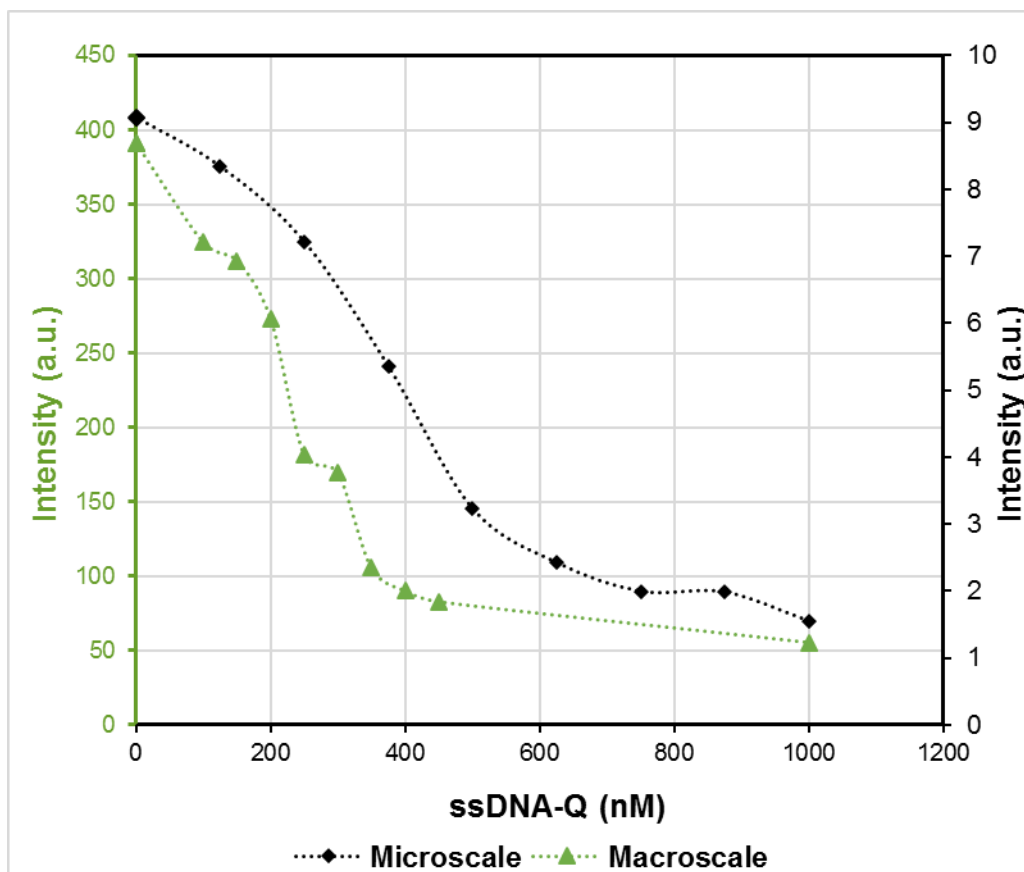


Figure 3.14. Comparison of Fluorescence for 500 nM of Aptamer and different concentrations of ssDNA-Q in Astrocytes Buffer in Micro and Macro scale.

3.3.2 Adenosine Behaviour in the Gradient Generator

With the PDMS working properly and the concentrations and intensity of Aptamer vs ssDNA-Q optimised, it is time to check the system by adding adenosine. In each inlet, the amount of Aptamer and ssDNA-Q (500 nM and 1000 nM respectively) is constant and the concentration of adenosine will vary. With these tests, an increase in fluorescence with adenosine is expected, since the binding between this purine and the Aptamer is more stable than the one established between Aptamer and ssDNA-Q. Since the behaviour of adenosine in the PDMS device is unknown, the concentration of adenosine chosen for the tests was high enough to ensure the system would be disturbed. A test was designed to understand the behaviour of Adenosine in the system. Figure 3.15 shows the concentrations used for each solution for the inlets and also the relative concentrations calculated to each chamber.

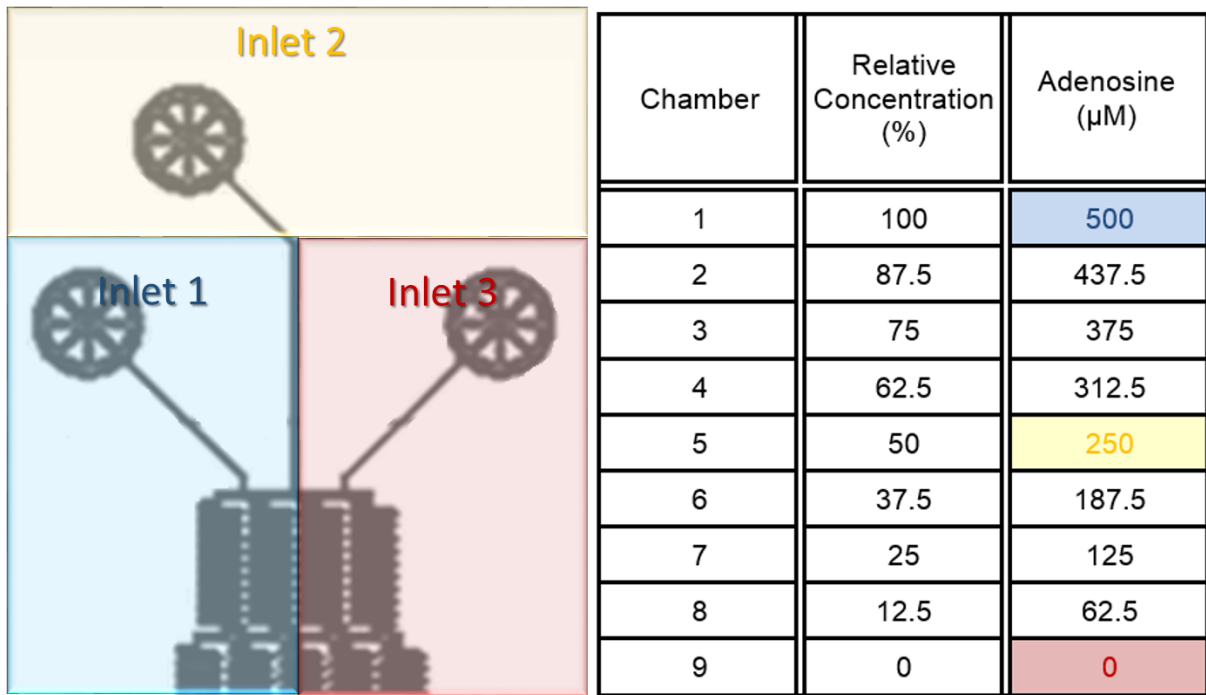


Figure 3.15. Relative concentration for each chamber of the PDMS device. The highlight cells of the table correspond to the concentration of adenosine from each solution prepared. All the three solutions contained the mix of 500 nM Aptamer and 1000 nM ssDNA-Q.

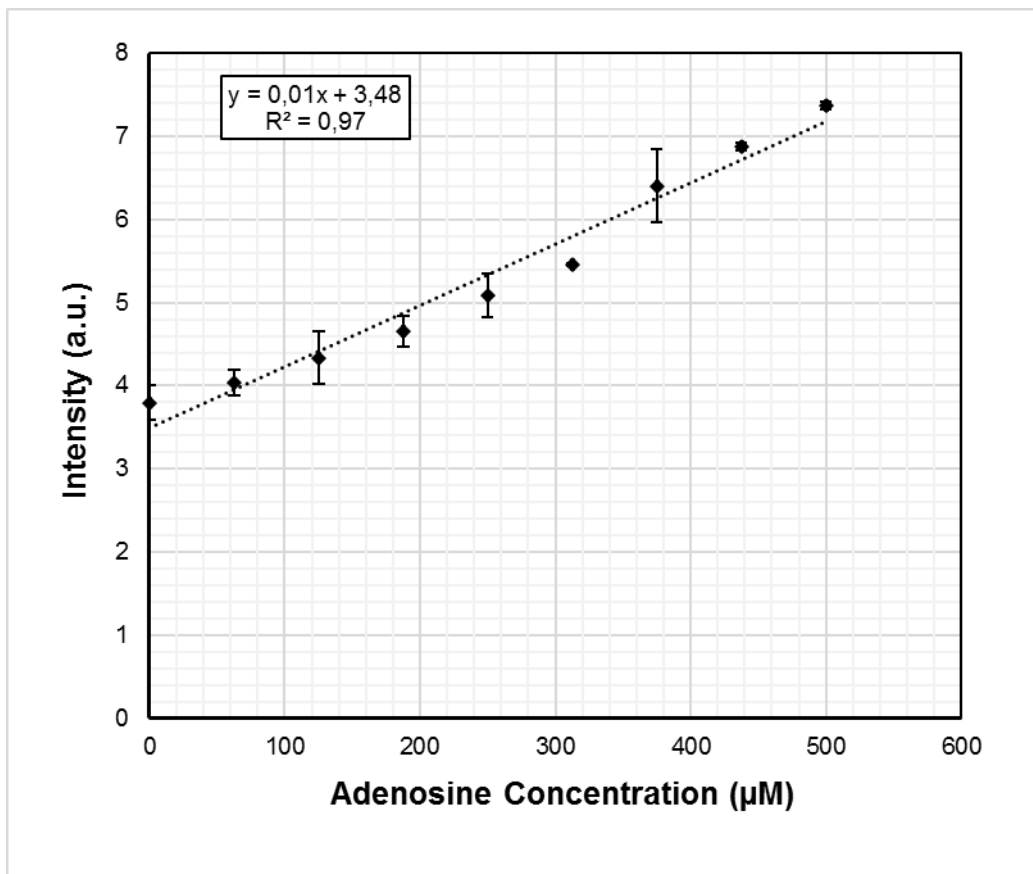


Figure 3.16. Intensity for different concentrations of Adenosine with 500 nM Aptamer and 1000 nM ssDNA-Q. Conditions of acquisition: 1s Exposure and 2x Gain

Analysing the data, the effect of adenosine is notorious. Comparing the results with the first test performed, with 500 nM Aptamer and various concentrations of ssDNA-Q, there are two results in focus: the intensity to 500 nM Aptamer without ssDNA-Q, from the first test without adenosine ($9.1 \text{ a.u.} \pm 0.3$) and the intensity to the mix 500 nM Aptamer+1000 nM ssDNA-Q with 500 μM adenosine ($7.4 \text{ a.u.} \pm 0.1$). This result proves a good binding between Aptamer and adenosine, since although in the second case, the quencher is present the intensity is high. In terms of behaviour of the molecules in a PDMS device, there are no concerns, due to this test.

In order to better understand which quantity of adenosine can be detected, the LoD was again calculated, using equation (5). For this experiment the LoD obtained was 81 μM , which represents an improvement compared to the results obtained in the previous section, although is far from the main goal of the work. The experiment was repeated, but now with lower concentrations of adenosine. Three solution were prepared to flow in each inlet with 500 nM Aptamer and 1000 nM ssDNA-Q and different concentrations of adenosine for each one: 0 μM , 125 μM and 250 μM . Again, the relative concentration for each chamber was calculated. The results from this experiment are below.

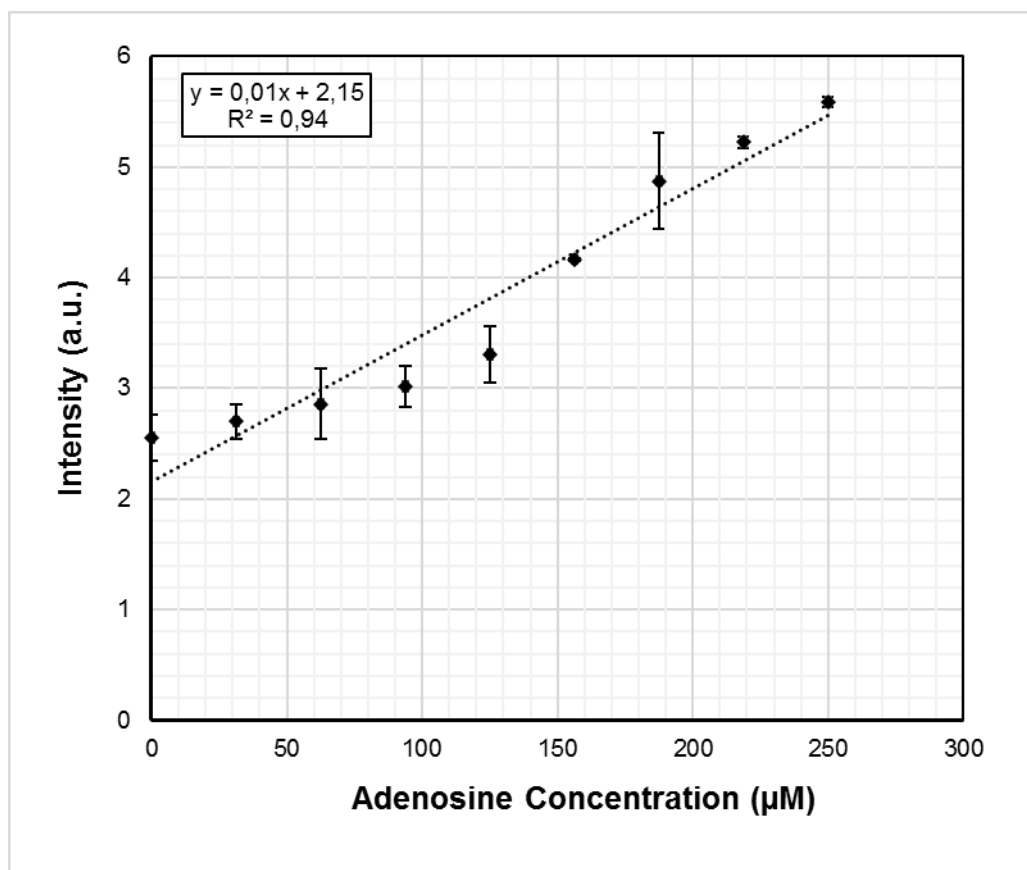


Figure 3.17. Intensity for different concentrations of Adenosine with 500 nM Aptamer and 1000 nM ssDNA-Q. Conditions of acquisition: 1s Exposure and 2x Gain

Again, and using the equation (5), the LoD for this experiment was calculated and the result obtained was 104 μM , which is higher than the one obtained before, which leads to a comparison between the graphs and bringing some concerns.

The difference in some common points between the experiments with adenosine is not very disturbing since this is in a small scale. In fact, to compare better the data points in common between both experiments, a new graph was designed, normalized to the value of 500 nM Aptamer (without ssDNA-Q and adenosine) and establish as 100% of the signal.

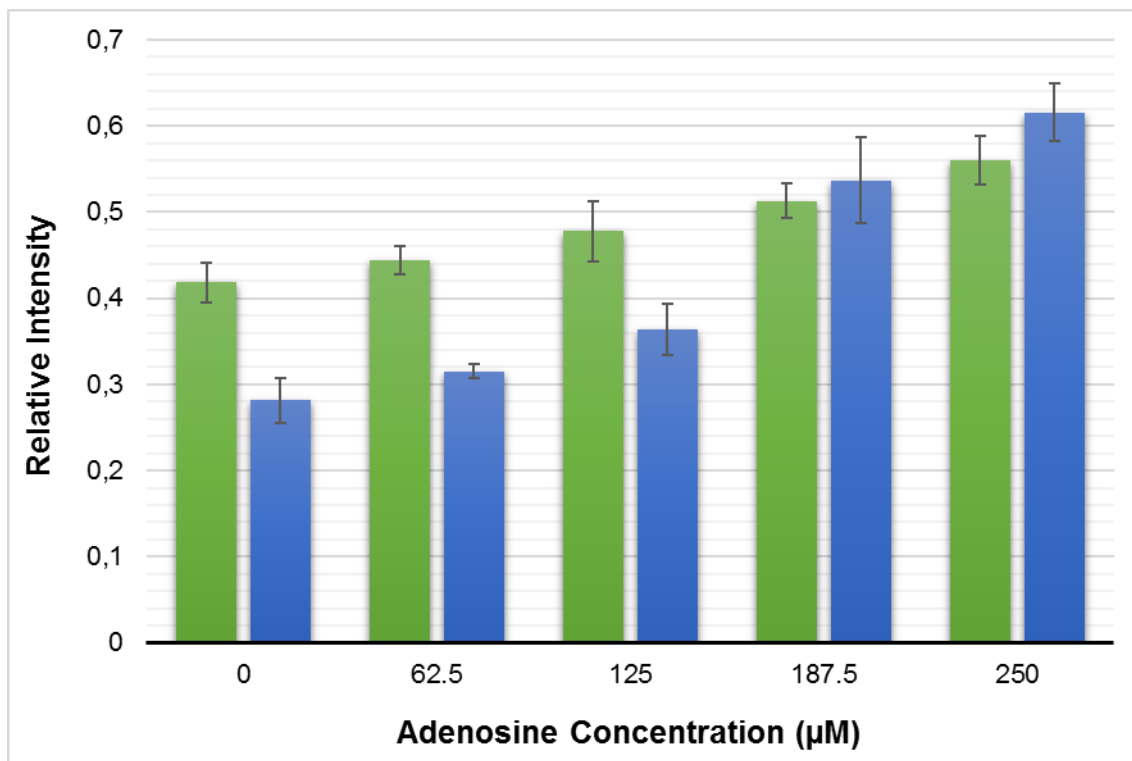


Figure 3.18. Comparison of the common relative concentrations of the two tests with Adenosine. The results are normalized to the intensity value of 500 nM Aptamer (without adenosine and ssDNA-Q).

The signal is slight different for the same relative concentrations in each experiment for same concentrations, in particular, the ones with lower concentration of adenosine and with the increase of adenosine the results are more similar. Since this is a gradient generator, the two concentrations of the Figure 3.18, which are from the solutions prepared are 0 µM and 250 µM of adenosine. This can indicate that one of the solutions was not properly prepared and affect the results. Furthermore, a quick analysis of the linear regression, in particular the coefficient of determination (R^2), performed for Figure 3.16 and Figure 3.17, give us a sense that the linear model is better for Figure 3.16 rather for Figure 3.17. With these results, there is a small approach to the main goal, and the desirable concentration of adenosine is closer, but is not enough.

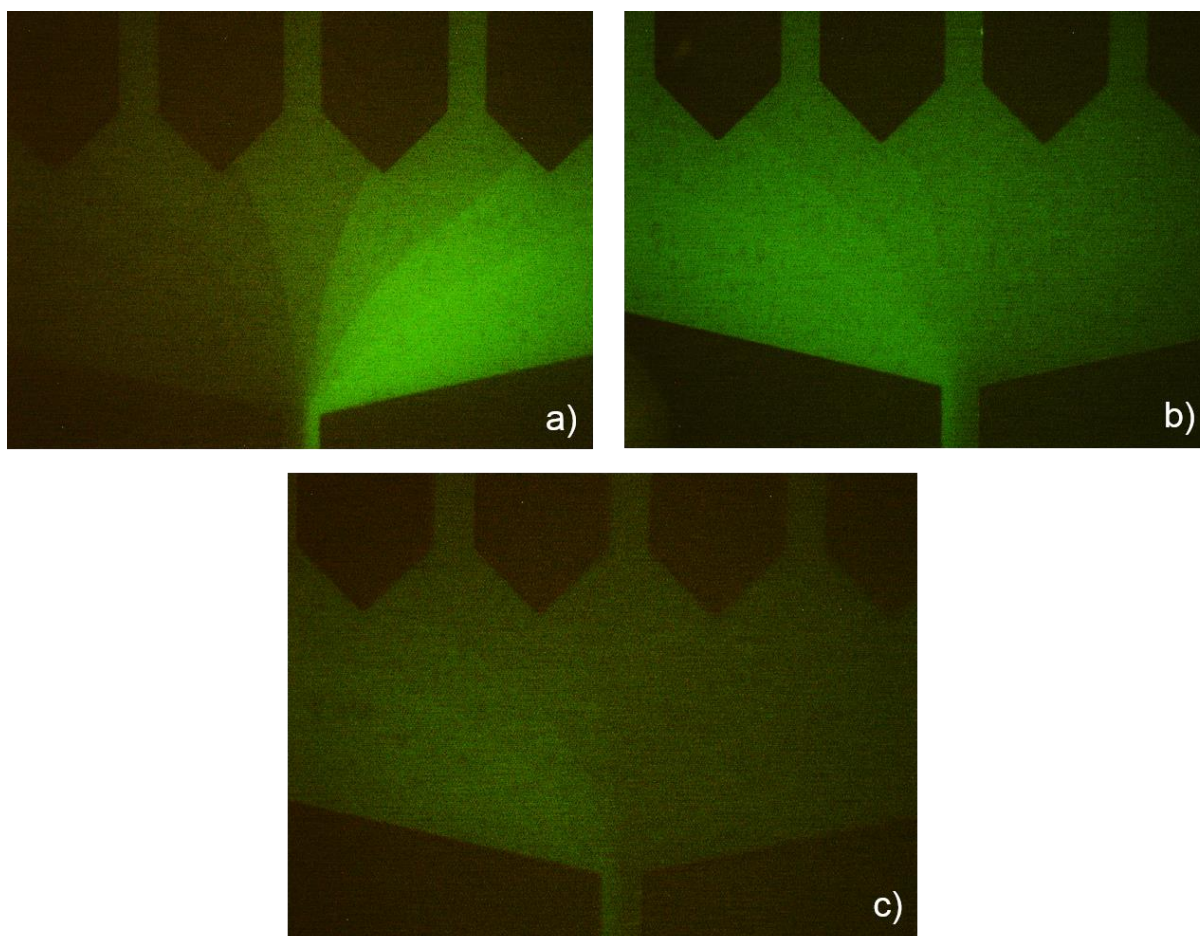


Figure 3.19. Outlets of PDMS Devices. a) Inlet 1: Aptamer (500 nM) + ssDNA-Q (1000nM) Inlet 2: Aptamer (500 nM) + ssDNA-Q (500 nM) Inlet 3: Aptamer (500 nM) b) 3 inlets with same concentration of Aptamer and ssDNA-Q (500 nM and 1000 nM) e different concentrations of adenosine (Inlet 1: 500 μ M; Inlet 2: 250 μ M; Inlet 3: 0 μ M) c) 3 inlets with same concentration of Aptamer and ssDNA-Q (500 nM and 1000 nM) e different concentrations of adenosine (Inlet 1: 250 μ M; Inlet 2: 125 μ M; Inlet 3: 0 μ M). Conditions of acquisition: 2x Gain and 1s Exposure.

In order to optimize the system and reduce the LoD, some factors have to be changed. Two of the factors were: the concentrations of Aptamer and ssDNA-Q and the conditions of acquisition in the microscope. The first factor aroused the important question of the ratio of numbers of molecules in the system. The ratio between Aptamer and ssDNA-Q was optimized, the ratio between Aptamer-ssDNA-Q and adenosine was not. Since this nucleoside is a very small molecule, the concentrations can influence the sensitivity of the system. The absolute fluorescence obtained for these experiments was low (Figure 3.19), resulting in a low range to allow the understanding of the behaviour of lower concentrations of adenosine, which may influence the detection limit.

Taking these concerns into account, new experiments were designed in order to optimize the system.

3.4 Towards physiological concentrations of adenosine in the Gradient Generator

Adenosine acts via diverse receptors, each one associated with a specific concentration which ranges between 1 nM and 20 μ M.

A comparison between this range of concentrations and the limit of detection obtained in the described experiments indicates that the system needs to be optimized to a limit detection in the order of μ M to be obtained. As mentioned in the previous section, there are some parameters which can be changed in order to optimize the system (the ratio of molecules between the mix Aptamer-ssDNA-Q and adenosine used may not be suitable and the conditions of acquisition might not be the most appropriate).

In the experiments previously described, solutions constituted by 500 nM of Aptamer and 1000 nM of ssDNA-Q were used, resulting in a detection limit of 81 μ M. Since this is a competitive system where adenosine competes with ssDNA-Q to bind the aptamer, an increase in the number of adenosine molecules in the system results in an increase in the number of adenosine molecules for each aptamer, and consequently more signal. Since the main objective is to reduce the detection limit, there is a need to change the concentration of the mix Aptamer and ssDNA-Q (maintaining the ratio between them). An increase in the number of adenosine molecules in solution, relatively to the number of molecules in the mix Aptamer-ssDNA-Q, is desirable; this can be achieved by decreasing the concentration of Aptamer and ssDNA-Q. This procedure would lead to another concern: conditions of acquisition. In the previous experiments, the range of intensity was low; by reducing the concentration of aptamer, the number of fluorophores will also be reduced and consequently so will the fluorescence intensity. A change in acquisition conditions is crucial. Until now, the acquisition conditions were: 1s Exposure and 2x Gain. Since a better signal and not a higher resolution is desired, the best option is to use a higher gain and a similar time of exposure (thus avoiding photobleaching – destruction of the fluorophores). Taking all these aspects into account, a new experiment was designed. For this new test, the concentrations of Aptamer and ssDNA-Q are reduced to - 125 nM Aptamer and various concentrations of ssDNA-Q – and the acquisition conditions changed for 2s Exposure and 5x Gain. The methods and materials used are the same as in the previous experiments. To understand how limited the range of intensity could be, the first test, was Aptamer and ssDNA-Q:

- Inlet 1: 125 nM Aptamer + 500 nM ssDNA-Q
- Inlet 2: 125 nM Aptamer + 250 nM ssDNA-Q
- Inlet 3: 125 nM Aptamer

As can be seen in the Figure 3.20, the signal is already too low and the background is too high which will induce more error.

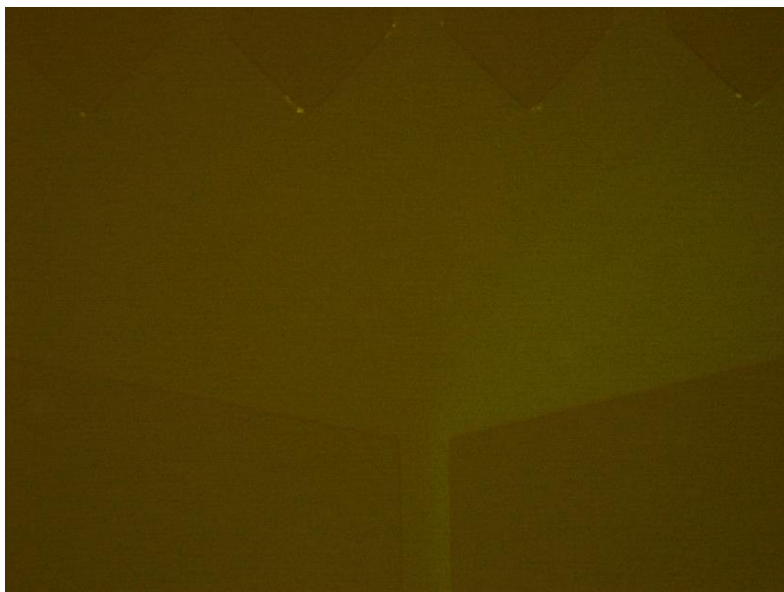


Figure 3.20. Outlet of PDMS Device, with 125 nM Aptamer and different concentrations of ssDNA-Q.

Comparing with macroscale results, this was expected, since for 100 nM Aptamer the signal was already considered weak, and in microscale that should reveal to be a problem.

Since this reduction of Aptamer and ssDNA-Q seems to be undue, it is considered a slight increase of the mix Aptamer-ssDNA-Q. The procedures described in Section 3.3 were followed, and the concentrations used for each test are presented in Figure 3.21.

		Test 1 - Control	Test 2	Test 3
Inlet 1	Aptamer (nM)	250	250	250
	ssDNA-Q (nM)	1000	500	500
	Adenosine	0	500	250
Inlet 2	Aptamer (nM)	250	250	250
	ssDNA-Q (nM)	500	500	500
	Adenosine (μ M)	0	250	125
Inlet 3	Aptamer (nM)	250	250	250
	ssDNA-Q (nM)	0	500	500
	Adenosine (μ M)	0	0	0

Figure 3.21. Concentrations of Aptamer, ssDNA-Q and adenosine for each test.

The acquisition conditions will be maintain (2s Exposure and 5x Gain), since higher values for any conditions can bring another kind of problems and influence negatively the intensity of fluorescence mostly because of photobleaching.

For each test, the concentrations in each chamber were calculated and are presented in Appendix. Under these new conditions, although the concentration of Aptamer + ssDNA-Q is smaller, a stronger signal is expected, due to the amplification of signal imposed by the gain.

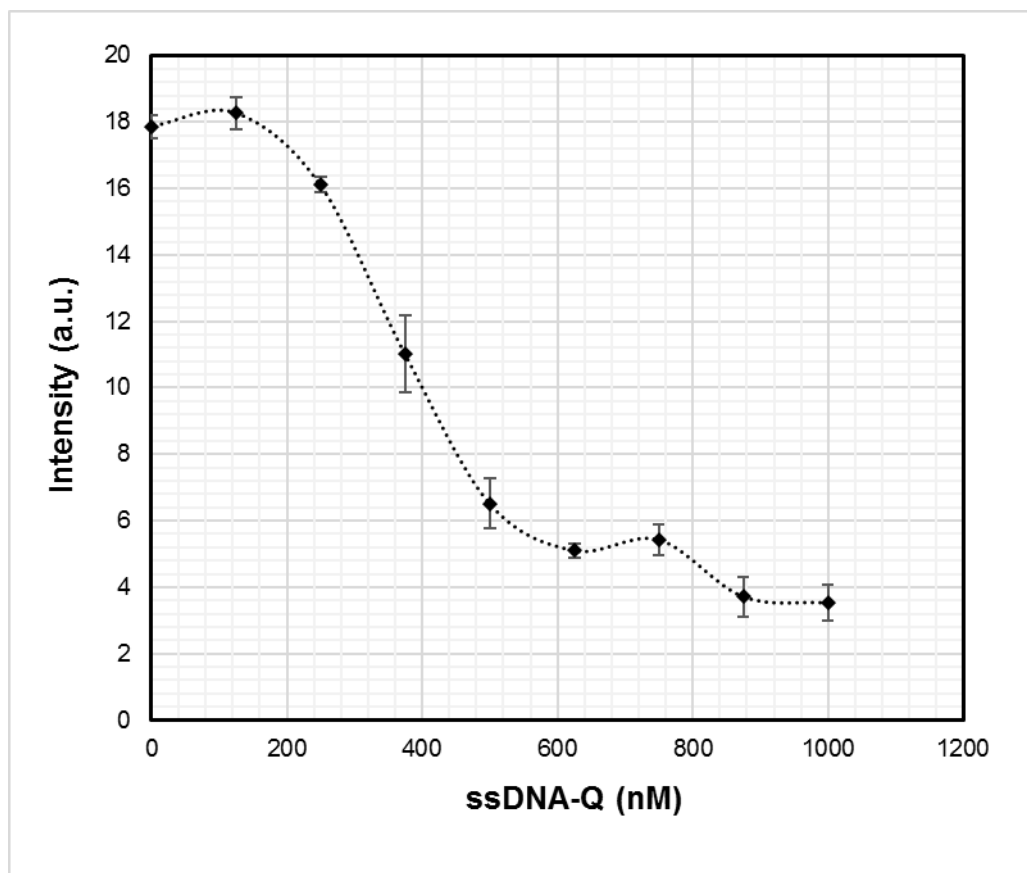


Figure 3.22. Fluorescence Intensity for 250 nM of Aptamer and various concentrations of ssDNA-Q, in PDMS device. Each point represents a different chamber. Acquisition conditions: 2s Exposure 5x Gain

Figure 3.22, shows the expected result. Comparing the intensity of 500 nM Aptamer (without ssDNA-Q or adenosine) from previous tests with the intensity of 250 nM Aptamer (without ssDNA-Q or adenosine) the difference is considerable:

- For 500 nM Aptamer the intensity is: 9.1 a.u. \pm 0.3
- For 250 nM Aptamer the intensity is: 17.9 a.u. \pm 0.4

There is a clear improvement of the signal when comparing the experiments. This was the expected behaviour, although the concentration of molecules was half in this new experiment, the acquisition conditions were very different, with a higher time exposure and a greater gain. Furthermore, these new results are coherent, and the linear regression is appropriate (the R^2 value is 0.90).

For the experiments with adenosine, already described, the results are presented in the next graph.

Comparing Figure 3.23 with Figure 3.16 and Figure 3.17, the first difference that can be detected is, the high intensity of the last graph presented. The reasons are the same already

explained for the comparison of graphs with Aptamer and ssDNA-Q. A brief comparison of the intensity of 250 nM Aptamer with 500 nM ssDNA-Q (3.7 ± 0.9) with the mix 250 nM Aptamer+500 nM ssDNA-Q and 500 μ M Adenosine (12.5 ± 0.5) can be reflected in an increase of approximately 70% of signal. Furthermore, since in these two experiments the results were consistent, the LoD was calculated using the points from the two experiments. For this experiment, the LoD was 95 μ M, which is not a desirable result.

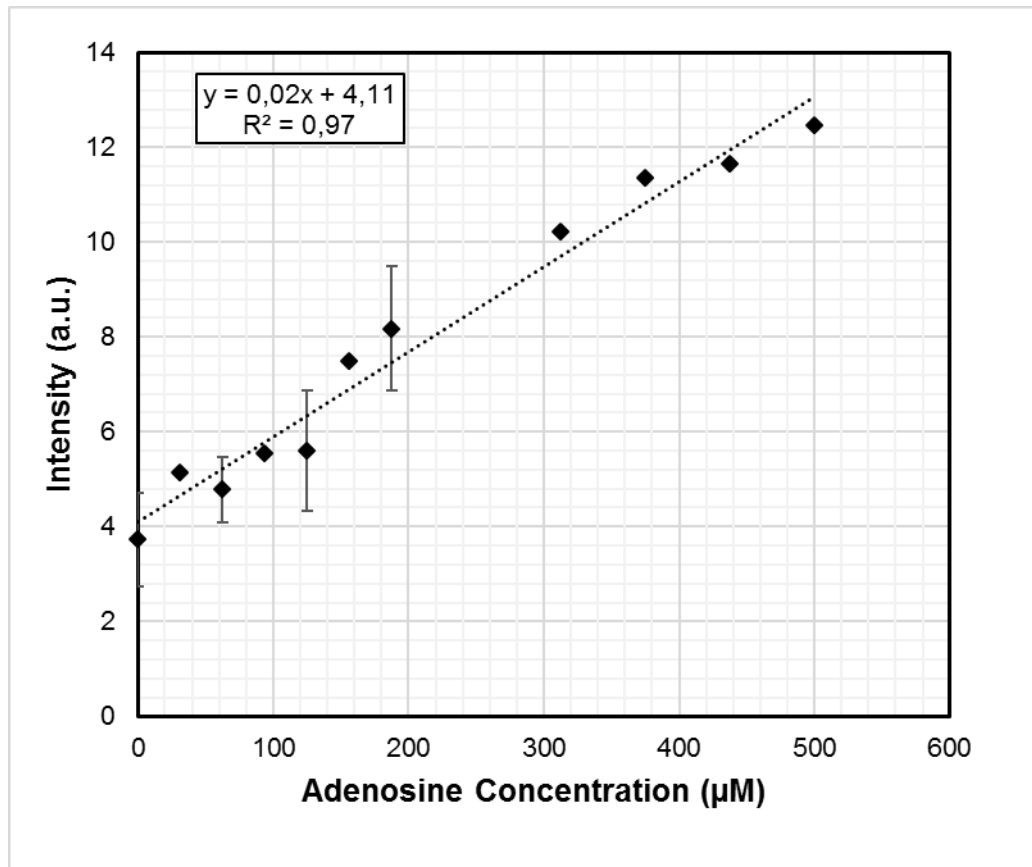


Figure 3.23. Intensity for different concentrations of Adenosine with 250 nM Aptamer and 500 nM ssDNA-Q. Conditions of acquisition: 2s Exposure and 5x Gain

There are many aspects that can be optimized in order to increase the signal besides the acquisition conditions. Rethinking new strategies or even an optimization of the PDMS device are the main concerns.

Since the PDMS device was re-used from another type of experiments, its optimization for this kind of experiment is crucial. The structure was designed to perform biological tests using cells, and was dimensioned for that purpose. The channels are very small in all dimensions, which means the area where the light strikes is considerable small, compared with standard straight microchannels. One option is to increase the height of the channels. This can be easily done when the fabrication of mould is done. But, since the behaviour between all the molecules is already known in PDMS structures, a good option is to use simpler channels and with the concentrations of interest only, instead of this method with 9 different concentrations.

Another important point is the way the acquisition was made. All the experiments in microscale were made in flow, i.e., the molecules were in constant movement, although in steady state. In this kind of work it is important to have a complete control on the molecules and the immobilization of the Aptamer must be a priority step.

And it is with immobilization in mind that in the next section a brief experiment and discussion will be made.

3.4.1 Immobilization of the Aptamer

The current approach to detecting adenosine adapted from (Elowe, et al., 2006) is composed by an aptamer labelled with a fluorophore and an ssDNA labelled with a dabcyI which quenches the signal, in the absence of adenosine. Until now, all the experiments were performed in solution, and none of the molecules were immobilized in a surface. Although the system implemented serves the propose of detecting adenosine, the sensitivity is not enough for the main challenge of this work, which is to achieve a detection limit in the order of μM . Immobilization, is then the next step to improve affinity and sensibility of the system. As previous explained in the theoretical introduction, there are many procedures to immobilize aptamers, based in immobilization of DNA. Since the Aptamer available are not properly labelled for an immobilization on a surface with, for example, biotin, the electrostatic immobilization seems to be the best procedure due to resources.

For this immobilization, and as described 2.2.4, a solution of aminopropyltriethoxy silane (APTES) was used, resulting in a monolayer of positively $-\text{NH}_2$ on the surface. Due to the negative charges of the phosphate groups of the Aptamer, an electrostatic force will be established with the positive charges of the amino groups, resulting in the immobilization of the Aptamer (Figure 3.24 a) and b)). With the Aptamer immobilized, the ssDNA-Q was flowed to the channel and then washed to remove all the molecules that did not bind with the Aptamer (Figure 3.24 c) and d)).

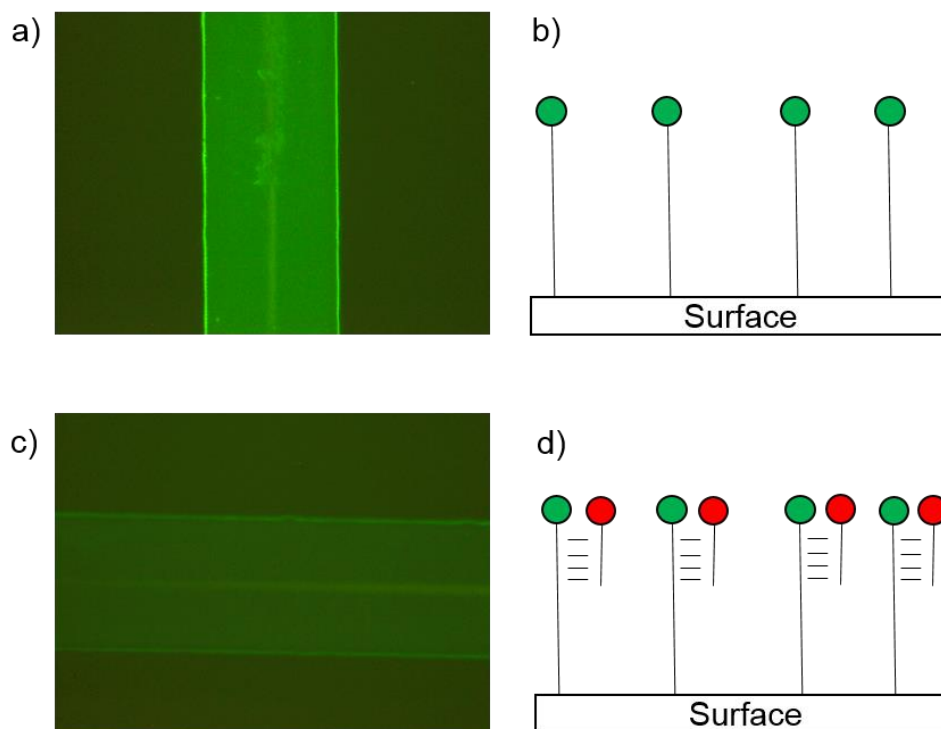


Figure 3.24. a) and b) Immobilization of the Aptamer and its Schematic. c) and d) Aptamer immobilized binding with ssDNA-Q and its schematic.

The decrease in fluorescence after adding ssDNA-Q to the immobilized aptamer is evident. An analysis of both pictures using ImageJ indicates that an intensity of 15.7 a.u. for the Aptamer and 3.8 a.u. for the mix Aptamer+ssDNA-Q was obtained. This represents a decrease of 76% in the signal, which means that the ssDNA-Q binds very well to the immobilized Aptamer. The interaction between Aptamer and ssDNA-Q is not affected by the electrostatic immobilization.

The last step of this experiment was to introduce the adenosine in the channel with a low flow rate (0.5 $\mu\text{L}/\text{min}$), and analyse the reactions in the channel in real time. Images were acquired in intervals of 20s for 5min in order to avoid photobleaching. After this period, the last image was analysed with ImageJ, indicating an intensity of 3.9 a.u., which is almost the same for the Aptamer+ssDNA-Q. This means that adenosine could not compete with ssDNA-Q and bind with the Aptamer, and in this way increase the signal. The failure of the binding between adenosine and the Aptamer is related to the procedure used for the immobilization. As reported by (Gueroui, Place, Freyssingéas, & Berge, 2002), for example, DNA-Protein interactions cannot be performed as the entire DNA strand is fixed to the substrate leaving little room. The same analysis can be applied to this system, since the Aptamer is entirely fixed to the substrate, which influences the structure of the aptamer, blocking the binding to the adenosine.

4 CONCLUSIONS AND FUTURE WORK

The first main conclusion of this work is that the system developed with the aptamer, can detect adenosine, although it needs some optimizations in the future.

The first conclusion from the experimental work is drawn from the design of the aptasensor, since the first experiments led to the conclusion that the best ratio between the Aptamer and ssDNA-Q, which permits the quenching of the fluorophore present in the Aptamer, is 1:2 (Aptamer: ssDNA-Q).

Under proper conditions, the designed aptasensor was capable of detecting adenosine, first in macroscale and then in a miniaturized system.

On both cases it was possible to verify that, although aptamers are presented with high affinity, there are aspects which can influence its proper functioning, such as the pH of the solution or the absence/presence of components (for example, salt).

In macroscale, the main conclusion inferred from the interaction between the aptasensor and adenosine was that, although the TE Buffer used proved to be the best option for storing both molecules of the aptasensor (Aptamer and ssDNA-Q), it was not appropriate to promote the binding of the Aptamer with adenosine. This may be due to the influence of the components of the buffer in the proper conformation of the aptamer to bind adenosine, which is crucial. Using the other two Buffers (HEPES and Astrocytes), the aptasensor worked: in the presence of adenosine, the aptamer binds to it instead of the ssDNA-Q, and there is an increase of signal. In terms of LoD, the difference for each Buffer was high (584 μM for HEPES Buffer and 354 μM for Astrocytes Buffer) and quite far from the main goal of this work, which is to detect physiological concentrations of adenosine in much lower concentrations. At this stage, it was also concluded that, for the next steps of the experimental work, the Astrocytes Buffer should be employed, due to the future work.

As for the microscale, the choice of a gradient generator for the first tests in microfluidic led to successful results: the tests were always very reproducible and it was possible to distinguish and quantify at the same time the intensity of the signal for different concentrations of adenosine. The first tests with adenosine brought a slightly better LoD (81 μM), compared to the ones obtained in the macroscale, but still far from the one needed. Based on these results, some conclusions were taken and used for the next steps of optimization of the system. The first conclusion is that the concentrations used for the mix Aptamer + ssDNA-Q probably were not appropriate. Additionally, the low range of signal indicated that the acquisition conditions were not the most appropriate.

The next set of tests took these facts into account and led to some interesting conclusions. Although lower concentrations of Aptamer and ssDNA-Q were used, a general improvement of intensity signal in the experiments was found (9.1 a.u. \pm 0.3 for 500 nM Aptamer and 17.9 \pm 0.4 for 250 nM Aptamer). This higher signal is justified by the optimized acquisition conditions.

Another conclusion is that the concentrations of Aptamer cannot be lower than 125 nM, since this is the limit of detection of the PDMS device used. Regarding adenosine detection, the LoD obtained (95 μM), was still far from the concentration of adenosine defined. The optimizations were not enough, and based on the results and in literature, the next obvious step seems to be the immobilization of the aptamer, promoting a better control and a refinement of the system. With the immobilization, the gradient generator no longer makes sense, and straight channels were used.

The type of immobilization chosen was electrostatic. The test proved that the aptamer can, in fact, be immobilized at the surface and bind with the ssDNA-Q, but nothing happened when adenosine was added to the system. This problem is related to the fact that the immobilization is electrostatic, causing the DNA chain of the Aptamer to be immobilized, which changes its conformation and hinders the adenosine to bind.

Furthermore, although the results do not correspond entirely to the expected, this work represents the first steps towards the development of a refined system, using an aptasensor, to detect adenosine.

There are many aspects of the experimental procedures which can be optimized. Although the gradient generator was useful for the first experiments in microfluidics, to understand the behaviour of the aptasensor and adenosine, in a next stage of the work this technique may be abandoned, since the immobilization of the aptamer seems to be the most feasible option for better control of the system. Taking this into consideration, the experiments should no longer be performed in flow.

As explained in Chapter 1, there are many reported techniques to immobilize the aptamer, which do not interfere with its conformation or high sensitivity. The technique that will better fit the system is the covalent immobilization, using biotin and streptavidin, already reported by (Huang & Liu, 2010).

For future work, it is proposed that the aptamer in addition to being labelled with FAM in 5'-end, is also labelled in 3' - end with biotin, in order to promote the immobilization through streptavidin. Furthermore, the system used for the detection is kept the same: hybridizing the aptamer with an ssDNA labelled with a quencher in 3' - end, suppressing the emission of the fluorophore and, in the presence of adenosine, the aptamer binds with it, releasing the ssDNA labelled with quencher, and the fluorescence signal increases. Due to the minimization of the effects of surface immobilization on the

binding of the aptamer, it should be introduced a spacer (five thymine nucleotides) between the aptamer and the biotin.

In what concerns the immobilization of the aptamer in the microfluidic device, the coating of the inner surface of the microfluidic channel with streptavidin, via long PEG (Polyethylene glycol) chain is proposed. Besides, the structure of the microfluidic device must be reconsidered, since the gradient generator no longer makes sense with the immobilization. For the first tests, straight normal channels, as the ones used in the experiments on the section 3.4.1 should be the best option.

With these optimizations, the system will be more consistent, stable and will allow sensitive and selective detection in small volumes.

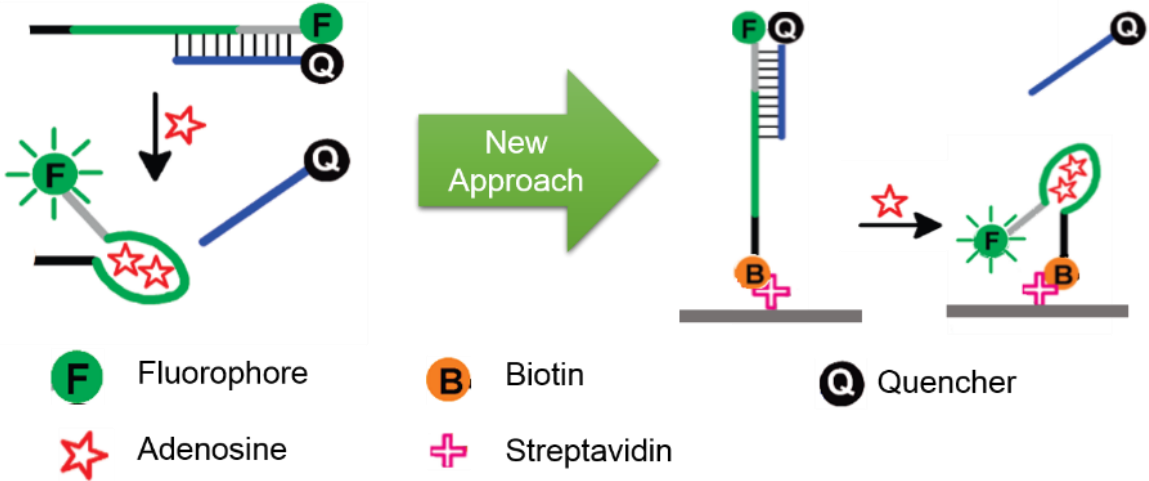


Figure 4.1. Actual Approach vs. Future Approach to detect adenosine.

BIBLIOGRAPHY

- Dertinger, S. K., Chiu, D. T., Jeon, N. L., & Whitesides, G. M. (2001). Generation of Gradients Having Complex Shapes Using Microfluidic Networks. *Analytical Chemistry*, *73*, 1240-1246.
- Fernandes, J., Gameiro, A., Tenreiro, S., Chu, V., & Outeiro, T. (2013). Deciphering the molecular basis for alpha-synuclein toxicity in yeast using microfluidics integrating single cell traps and a chemical gradient generator.
- Aronicaa, E., Sandau, U., Iyer, A., & Boison, D. (2013). Glial adenosine kinase – A neuropathological marker of the epileptic. *Neurochemistry International*, *63*, 688–695.
- Balamurugan, S., & Obubuafo, A. (2007). Surface immobilization methods for aptamer diagnostic applications. *Analytical and Bioanalytical Chemistry*, *390*, 1009–1021.
- Boison, D. (2012). Adenosine Dysfunction in Epilepsy. *Glia*, *60*, 1234–1243.
- Chikahisa, S., & Séi, H. (2011). The role of ATP in sleep regulation. *Frontiers in Neurology*, *2*.
- Diógenes, M., Neves-Tomé, R., Fucile, S., Martinello, K., Scianni, M., Theofilas, P., & Sebastião, A. (2014). Homeostatic Control of Synaptic Activity by Endogenous Adenosine is Mediated by Adenosine Kinase. *Cerebral Cortex*, *24*, 67-80.
- Dollins, C. M., Nair, S., & Sulle, B. A. (2008). Aptamers in Immunotherapy. *Human Gene Therapy*, *19*, 443-450.
- Ellington, A. D., & Szostak, J. W. (1990). In vitro selection of RNA molecules that bind specific ligands. *Nature*, *346*, 818 - 822.
- Elowe, N. H., Nutiu, R., Allali-Hassani, A., Cechetto, J. D., Hughes, D. W., Li, Y., & Brown, E. D. (2006). Small-Molecule Screening Made Simple for a Difficult Target with a Signaling Nucleic Acid Aptamer that Reports on Deaminase Activity. *Angewandte Chemie Int. Ed.*, *45*, 5678-5652.
- Feng, C., Dai, S., & Wang, L. (2014). Optical aptasensor for quantitative detection of small biomolecules: A review. *Biosensors and Bioelectronics*(59), 64-74.
- Fredholm, B. B., Ijzerman, A. P., Jacobson, K. A., Klotz, K.-N., & Linden, J. (2001). Nomenclature and Classification of Adenosine Receptors. *Pharmacological Reviews*, *53*, 527-552.
- Gameiro, A. (2013). *Microfluidic Systems for Studies in Parkinson's Disease*. Lisbon.
- Gomes, C., Kaster, M. P., Tomé, A. R., Agostinho, P., & Cunha, R. (2011). Adenosine receptors and brain diseases: Neuroprotection and neurodegeneration. *Biochimica et Biophysica Acta*, *1808*, 1380–1399.
- Gopinath, S. C. (2007). Methods developed for SELEX. *Analytical and Bioanalytical Chemistry*, *387*, 171-182.

- Gueroui, Z., Place, C., Freyssingas, E., & Berge, B. (2002). Observation of fluorescence microscopy of transcription on single combed DNA. *Proceedings of the National Academy of Sciences*, *99*, 6005-6010.
- Halperin, A., Buhot, A., & Zhulinay, E. (2005). Brush Effects on DNA Chips: Thermodynamics, Kinetics, and Design Guidelines. *Biophysical Journal*, *89*, 796–811.
- Huang, P.-J. J., & Liu, J. (2010). Flow Cytometry-Assisted Detection of Adenosine in Serum with an Immobilized Aptamer Sensor. *Analytical Chemistry*, *82*, 4020–4026.
- Huang, D.-W., Niu, C.-G., Zeng, G.-M., & Ruan, M. (2011). Time-resolved fluorescence biosensor for adenosine detection based on home-made europium complexes. *Biosensors and Bioelectronics*, *29*, 178–183.
- Huizenga, D. E., & Szostak, J. W. (1995). A DNA aptamer that binds adenosine and ATP. *Biochemistry*, *34*, 656-665.
- Jain, K. (2008). *The Handbook of Nanomedicine*. Human Press.
- Jarvis, S. M., & Young, J. D. (1986). Nucleoside Transport in Rat Erythrocytes: Two Components with Differences in Sensitivity to Inhibition by Nitrobenzylthioinosine and p-Chloromercuriphenyl Sulfonate. *The Journal of Membrane Biology*, *93*, 1-10.
- Jeon, N. L., Dertinger, S. K., Chiu, D. T., Choi, I. S., Stroock, A., & Whitesides, G. M. (2000). Generation of Solution and Surface Gradients Using Microfluidic Systems. *Langmuir*, *16*, 8311-8316.
- Juskowiak, B., Galezowska, E., Zawadzka, A., Gluszynska, A., & Takenaka, S. (2006). Fluorescence anisotropy and FRET studies of G-quadruplex formation in presence of different cations. *Spectrochimica Acta Part A*, *64*, 835–843.
- Lee, J.-O., So, H.-M., Jeon, E.-K., Chang, H., Won, K., & Kim, Y. (2008). Aptamers as molecular recognition elements for electrical nanobiosensors. *Analytical and Bioanalytical Chemistry*, *390*, 1023–1032.
- Li, L.-L., Ge, P., Selvin, P., & Lu, Y. (2012). Direct Detection of Adenosine in Undiluted Serum Using a Luminescent Aptamer Sensor Attached to a Terbium Complex. *Analytical Chemistry*, *84*, 7852–7856.
- Lim, Y., Kouzani, A., & Duan, W. (2009). Aptasensors Design Considerations. *Communications in Computer and Information Science*, *51*, 118-127.
- Liss, M., Petersen, B., Wolf, H., & Prohaska, E. (2002). An Aptamer-Based Quartz Crystal Protein Biosensor. *Analytical Chemistry*, *74*, 4488-4495.
- Mascini, M. (2009). *Aptamers in Bioanalysis*. United States of America: John Wiley & Sons, Inc.
- Misra, V. K., Sharp, K. A., Friedman, R. A., & Honig, B. (1994). Salt Effects on Ligand-DNA Binding. *Journal of Molecular Biology*, *245*-263.
- Newby, A. (1991). Adenosine: Origin and Clinical Roles. *Advances in Experimental Medicine and Biology*, *309A*, 265-270.
- Patel, M., Dutta, A., & Huang, H. (2011). A selective adenosine sensor derived from a triplex DNA aptamer. *Analytical and Bioanalytical Chemistry*, *400*, 3035–3040.
- Porkka-Heiskanena, T., & Kalinchuk, A. (2011). Adenosine, energy metabolism and sleep homeostasis. *Sleep Medicine Reviews*, *15*, 123-135.

- Ribeiro, J. A., Sebastião, A. M., & de Mendonça, A. (2003). Adenosine receptors in the nervous system: pathophysiological implications. *Progress in Neurobiology*(68), 377-392.
- Sassolas, A., Blum, L., & Leca-Bouvier, B. (2011). Optical detection systems using immobilized aptamers. *Biosensors and Bioelectronics*, 26, 3725–3736.
- Schutze, T., Wilhelm, B., Greiner, N., Braun, H., Peter, F., & Morl, M. (2011). Probing the SELEX Process with Next-Generation Sequencing. *Plos One*, 6(12).
- Scullion, M., Krauss, T., & Di Falco, A. (2013). Slotted Photonic Crystal Sensors. *Sensors*, 13, 3675-3710.
- Sebastião, A. M., & Ribeiro, J. A. (2000). Fine-tuning neuromodulation by adenosine. *TIPS* 21, 341-346.
- Sebastião, A. M., & Ribeiro, J. A. (2009). Adenosine Receptors and Central Nervous System. Em *Handbook of Experimental Pharmacology* (Vol. 193, pp. 471-534).
- Sia , S., & Whitesides, G. (2003). Microfluidic devices fabricated in Poly(dimethylsiloxane) for biological studies. *Electrophoresis*, 24(21), 3563–3576.
- Smuca, T., Ahnb, I.-Y., & Ulrichb, H. (2014). Nucleic acid aptamers as high affinity ligands in biotechnology and biosensorics. *Journal of Pharmaceutical and Biomedical Analysis*, 210-217.
- Song, K.-M., Lee, S., & Ban, C. (2012). Aptamers and Their Biological Applications. *Sensors*, 32, 612-631.
- Stoltenburg, R., Reinemann, C., & Strehlitz, B. (2007). SELEX—A (r)evolutionary method to generate high-affinity nucleic acid ligands. *Biomolecular Engineering*, 24, 381-403.
- Strehlitz, B., Nikolaus, N., & Stoltenburg, R. (2008). Protein Detection with Aptamer Biosensors. *Sensors*, 8, 4296-4307.
- Tabling, P. (2003). *Introduction to Microfluidics*. New York: Oxford University Press.
- Toepkea, M., & Beebe, D. (2006). PDMS absorption of small molecules and consequences in microfluidic applications. *Lab on a chip*, 6, 1484-148.
- Tuerk , C., & Gold, L. (1990). Systematic evolution of ligands by exponential enrichment: RNA ligands to bacteriophage T4 DNA polymerase. *Science*, 249, 505-510.
- Xia, Y., & Whitesides, G. (1998). Soft Lithography. *Annual Review of Materials Science*, 28, 153-184.

APPENDIXES

Chamber	Relative Concentration (%)	ssDNA-Q (nM)	Adenosine (μ M)	
		Test 1	Test 2	Test 3
1	100	1000	500	250
2	87.5	875	437.5	218.75
3	75	750	375	187.5
4	62.5	625	312.5	156.25
5	50	500	250	125
6	37.5	375	187.5	93.75
7	25	250	125	62.5
8	12.5	125	62.5	31.25
9	0	0	0	0

Appendix 1. Concentrations calculated to each chamber, from each test. In both three tests there is the same concentration of Aptamer (250 nM), Test 1 does not have adenosine just ssDNA-Q and Test 2 and 3 have the same concentration of ssDNA-Q (500 nM) and differ